Linear Programming to Determine Molecular Orientation at Surfaces through Vibrational Spectroscopy

by

Fei Chen
B.Sc., University of Victoria, 2017

A Dissertation Submitted in Partial Fulfillment of the
Requirements for the Degree of

MASTER OF SCIENCE

in the Department of Computer Science

Linear Programming to Determine Molecular Orientation at Surfaces through Vibrational Spectroscopy

by

Fei Chen
B.Sc., University of Victoria, 2017

Supervisory Committee

Dr. Ulrike Stege, Co-Supervisor
(Department of Computer Science)

Dr. Dennis Hore, Co-Supervisor
(Department of Chemistry)

Supervisory Committee

Dr. Ulrike Stege, Co-Supervisor
(Department of Computer Science)

Dr. Dennis Hore, Co-Supervisor
(Department of Chemistry)

ABSTRACT

Applying linear programming to spectroscopy techniques, such as IR, Raman and SFG, is a new approach to extract the molecular orientation information at surfaces. Research has shown the computational gain when using the linear programming approach. However, linear programming approach does not always return the known molecular orientation distribution information when mock spectral information is applied to the linear programming model. The goal of my study is to figure out the reason that causes the failure. To achieve this goal, a simplified molecular model is designated to study the nature of the linear programming model. With the information gained, I further apply the linear programming approach to various cases in order to verify whether it can be systematically applied in different circumstances.

Contents

List of Tables

List of Figures

ACKNOWLEDGEMENTS

I would like to thank:

My husband, for supporting me in the low moments.

Dr. Ulrike Stege, for all the support, encouragement, inspiration and patience. I can only finish my thesis with her all help and courage.

Dr. Dennis Hore, for always giving me new ideas and wonderful discusses.

Kuo Kai Hung, for previous working and information sharing.

PITA and Dennis groups, for all the fun and knowledge we share in our weekly meeting.

I believe I know the only cure, which is to make one's centre of life inside of one's self, not selfishly or excludingly, but with a kind of unassailable serenity-to decorate one's inner house so richly that one is content there, glad to welcome any one who wants to come and stay, but happy all the same in the hours when one is inevitably alone.

Edith Wharton

Chapter 1

Introduction

1.1 Background and Motivation

A surface is what forms a common boundary between two phases of matter. The phases of matter can be of any forms, i.e, solid, liquid, and gas. The behavior of a surface greatly affects the properties of a material, such as oxidation, corrosion, chemical activity, deformation and fracture, surface energy and tension, adhesion, bonding, friction, lubrication, wear and contamination. Therefore, surface characterization identification remains an active area of research in the physics, chemistry, and biotechnology communities as well as in modern electronic technology. It also plays a crucial role in surface science. Among various surface properties, molecular orientation is a key factor of all, because molecular orientation greatly affects molecules' surface properties in aspects such as: adhesion, lubrication, catalysis, bio-membrane functions and so on. [10]

Many experimental techniques have been applied in the study of molecular orientation at surfaces. Among them the optical methods are more preferable. Such methods include infrared (IR) absorption, Raman scattering and visible-infrared sum-frequency generation (SFG) spectroscopies. All these vibrational spectra carry quantitative structural information of molecules at surfaces. Although each of them has its own strengths and shortcomings, they all share the following advantages when compared with other non-optical methods. First of all, they all can be applied to any surfaces accessible by light. Second, they are non-destructive. Third, they offer good spatial, temporal and spectral resolutions [2], [10]. An important advantage of

SFG techniques is that it can discriminate against bulk contributions. This means that its result will not take the effect from the bulk. In order to extract the quantitative structural information that molecules carry at surfaces, different spectroscopy techniques and analysis are required. Combining different spectroscopy techniques is a very effective way to achieve the goal of molecular orientation study at surfaces. However, finding the most effective ways to combine these techniques may not be clear.

In order to analyze these vibrational spectra, various factors need to be considered. For example, a molecule's vibrational mode in the molecular frame, the orientation average of the molecules adsorbed onto the surface based on the mathematical orientation distribution function and projecting the vibrational mode properties from molecular frame to laboratory frame. The main focus of my study is combining Linear Programming (LP) with different spectral information to obtain molecular orientation distribution at surfaces. In this thesis, I will explore how LP can facilitate extracting quantitative structural information of molecules at surfaces.

My approach is to first study our LP model's properties by applying it to a simplified molecule. After that, the LP model is applied to the representatives of realistic molecules to further explore the possibilities of our LP model. The realistic molecules that I am considering are six amino acids: methionine (Met), leucine (Leu), isoleucine (Ile), alanine (Ala), threonine (Thr) and valine (Val).

Before introducing the LP model and the molecule orientation studies, the basic theory of the IR, Raman and SFG spectra is introduced.

1.2 Experimental Probes: IR, Raman, SFG Vibrational Spectroscopy

Vibrational spectra are produced by the changes of a molecule's dipole moment and polarizability. The dipole moment and polarizability are changing as the molecule's conformation is changing.

IR is the absorption of passing infrared light through a sample at each frequency, which can be expressed by Equation 1.1.

$$A_{\mathrm{IR}} = -log_{10}\left(\frac{I}{I_o}\right) \tag{1.1}$$

where A_{IR} is the measured IR absorbance. I is the light intensity after infrared light pass through the sample. I_o is the initial light intensity.

The physical principle of IR spectra is the variation of the dipole moment μ (the first rank tensor) along the normal coordinates Q: $^{\partial\mu}/_{\partial Q}$. IR spectra can be further expanded by Equation 1.2.

$$A_{\mathrm{IR}} \approx \left|\frac{1}{\sqrt{2m_q w_q}}\frac{\partial\mu}{\partial Q}\right|^2 \tag{1.2}$$

where m_q is the reduced mass of the normal mode, and w_q is the resonance frequency. The dipole moment μ is a vector of x, y and z. The dipole moment derivatives can be expressed as Equation 1.3. The IR spectra can be obtained from 3 polarizations: x, y, z.

$$\frac{\partial\mu}{\partial Q} = \begin{bmatrix}\frac{\partial\mu_x}{\partial Q}\\ \frac{\partial\mu_y}{\partial Q}\\ \frac{\partial\mu_z}{\partial Q}\end{bmatrix} \tag{1.3}$$

In the Raman process, stocks-shifted light may be scattered from a molecule sample. Unlike IR, Raman spectra relate to the variation of the molecular polarizability α (the second rank tensor) along the normal coordinates Q: $^{\partial\alpha}/_{\partial Q}$.

$$I_{\mathrm{Raman}} \approx \left|\frac{1}{\sqrt{2m_q w_q}}\frac{\partial\alpha^{(1)}}{\partial Q}\right|^2 \tag{1.4}$$

where m_q and w_q are the same as defined in Equation 1.2. The polarizability is coupled with x, y, z components of the driving field and x, y, z components of the

induced polarization. Therefore, there are 9 elements in the polarizability, which can be expressed as Equation 1.5. It results in 9 polarizations of Raman spectra: xx, yy, zz, xy, xz, yx, yz, zy and zx.

$$\frac{\partial \alpha^{(1)}}{\partial Q} = \begin{bmatrix} \frac{\partial \alpha_{xx}^{(1)}}{\partial Q} & \frac{\partial \alpha_{xy}^{(1)}}{\partial Q} & \frac{\partial \alpha_{xz}^{(1)}}{\partial Q} \\ \frac{\partial \mu_{yx}}{\partial Q} & \frac{\partial \alpha_{yy}^{(1)}}{\partial Q} & \frac{\partial \alpha_{yz}^{(1)}}{\partial Q} \\ \frac{\partial \mu_{zx}}{\partial Q} & \frac{\partial \alpha_{zy}^{(1)}}{\partial Q} & \frac{\partial \alpha_{zz}^{(1)}}{\partial Q} \end{bmatrix} \tag{1.5}$$

SFG stands for sum frequency generation vibrational spectroscopy. SFG is a surface-specific technique. It is a non-linear optical process. SFG is the variation of the outer product of dipole moment and polarizability, $\alpha^{(2)}$ (the third rank tensor): $\frac{\partial \mu}{\partial Q} \otimes \frac{\partial \alpha}{\partial Q}$. Therefore, there are 27 elements for SFG spectra, which result in 3 unique polarizations of SFG spectra: xxz, xzx, and zzz.

$$I_{\text{SFG}} \approx \left| \alpha_{ijk}^{(2)} \right|^2 = \left| \frac{1}{2 m_Q w_Q} \left(\frac{\partial \alpha_{ij}^{(2)}}{\partial Q} \otimes \frac{\partial \mu_k}{\partial Q} \right) \right|^2 \tag{1.6}$$

1.3 Linear Programming

LP problems are optimization ones of a specific form. The standard form of LP is a minimization problem that has an objective function and a number of constraints as shown in Equation 1.7 [5]:

$$\begin{aligned} \text{minimize} \quad & c_1 x_1 + c_2 x_2 + ... + c_n x_n \\ \text{subject to} \quad & a_{11} x_1 + a_{12} x_2 + ... + a_{1n} x_n = \quad b_1 \\ & a_{21} x_1 + a_{22} x_2 + ... + a_{2n} x_n = \quad b_2 \\ & \qquad \vdots \qquad\qquad\qquad\quad \vdots \\ & a_{m1} x_1 + a_{m2} x_2 + ... + a_{mn} x_n = \quad b_m \\ & x_1 \geq 0, x_2 \geq 0, ..., x_n \geq 0, \end{aligned} \tag{1.7}$$

Food	Carrot	Cabbage	Cucumber	Required per dish
Vitamin A [mg/kg]	35	0.5	0.5	0.5mg
Vitamin C [mg/kg]	60	300	10	15mg
Dietary Fiber [g/kg]	30	20	10	4g
price[$/kg]	0.75	0.5	0.15	-

Table 1.1: Sample input of the diet problem

where x_i are the decision variables, a_{ij} is a matrix of known coefficients, b_i and c_i are vectors of known coefficients. The expression to be minimized is called objective function. The equalities and the inequalities are the constraints that all the decision variables need to subject to. These constraints specify a convex polytope that the objective function need to optimize over.

The diet problem is a popular example to illustrate the concept of LP. It is described as follows: a restaurant would like to achieve the minimal nutrition requirements with the lowest price over some food selections as shown in Table 1.1. For each meal, the minimum requirements for vitamin A, vitamin C and dietary fiber are 0.5mg, 15mg and 4g. The restaurant has three food options: raw carrot, raw white cabbage and pickled cucumber. The table also displays the nutrition content and the price of each ingredient. With all the information, we want to know how much carrot, cabbage and cucumber is needed in each meal, so that the minimal nutrition requirements can be met with the lowest price. In summary, the goal is to minimize the price, and the constraints are the nutrition requirements. Therefore, the following LP model is formulated as shown in Equations from 1.8 to 1.14.

$$\begin{aligned}
\text{minimize} \quad & 0.75x_1 + 0.5x_2 + 0.15x_3 && (1.8)\\
\text{subject to} \quad & 35x_1 + 0.5x_2 + 0.5x_3 \geq 0.5 && (1.9)\\
& 60x_1 + 300x_2 + 10x_3 \geq 15 && (1.10)\\
& 30x_1 + 20x_2 + 10x_3 \geq 4 && (1.11)\\
& x_1 \geq 0 && (1.12)\\
& x_2 \geq 0 && (1.13)\\
& x_3 \geq 0 && (1.14)
\end{aligned}$$

where x_1, x_2 and x_3 are the decision variables. Each decision variable presents the amount of each ingredient. Equation 1.8 is the objective function to minimize. Equation 1.9 to Equation 1.11 describe the nutrition requirements. Equation 1.12 to Equation 1.14 ensure the amount of each ingredient to be greater than 0. The coefficients in the objective function represent c_i vector in Equation 1.1. The coefficients of the decision variables in Equation 1.9, 1.10 and 1.11 represent a_{ij} matrix. b_i vector is composed by the right-hand side of Equation 1.9, 1.10 and 1.11.

In order to apply simplex method, the above LP problem needs to transfer into its standard form. The inequalities of Equations from 1.9 to 1.11 need to transform to equalities. Therefore, a new variable, called a slack variable (SV) is introduced to change each inequality to equality [1].

With the existing LP solvers that implemented simplex method, the optimal solution can be obtained within a second.

For a LP problem, there are only three kinds of solutions: feasible and bounded, feasible and unbounded, and infeasible. If the solution space is feasible and bounded, then there is one optimum solution. If it is feasible but unbounded, then there is a solution space with an infinite number of optimal solutions [3].

A general LP problem can be a minimization or maximization problem. Its constraints can be equalities or inequalities. For each non-standard LP problem, there are ways to convert it into its standard form. Furthermore, for a LP problem that contains n decision variables, its solution would be in a n-dimensional space called R^n. Each constraint is a hyperplane. It divides the R^n space into two half-spaces. Therefore, all the constraints together cut this R^n space into a convex polyhedron when there are feasible solutions. This makes LP a convex problem. The benefit of a convex problem is that the local optimal solution is the global optimum. LP solvers return the optimal solution. If a LP problem has a unique optimal solution, this solution is a vertex of the convex polyhedron. In other words, LP is a convex, deterministic process. It is guaranteed to converge to a single global optimum if there is a bounded solution space.

Another advantage of LP is that it can deal with tens or hundreds of thousands

of variables, which makes it suitable for the study of a molecule's orientation distribution at surfaces. Furthermore, LP problems are intrinsically easier to solve than many non-linear problems.

Various algorithms are available in solving LP problems, such as: simplex algorithm, interior point, and path-following algorithms. Both interior point and simplex are common and mature algorithms that work well in practice. Simplex is comparatively easier to understand and implement than interior point. Simplex method takes the advantage of the geometric concept that it visits the vertices of the feasible set (convex polyhedron), and checks the optimal solution among each visited vertex. The converging approach is different for these two methods. If there are n decision variables, usually simplex method converges in $O(n)$ operations with $O(n)$ pivots. Interior point traverses the edges between vertices on a polyhedral set. Generally speaking, Interior point method is faster for larger problems with sparse matrix. However, when experimenting with these two methods, the speed of them is not much different from each other for my study. In my study, simplex method has proved to be efficient and effective, and it is used for all the test cases.

Last but not the least advantage of LP is its speed. For any LP problem, if it has an optimal solution, this solution is always a vertex. Simplex method is based on this insight, namely that it starts at a vertex, then pivot from vertex to vertex, until it reaches the optimum. Although it has been shown that simplex method is not a polynomial algorithm, in practice it usually takes $2n \sim 3n$ steps to solve a problem (n is the number of the decision variables). Currently there are two main approaches in studying the orientation distribution of molecules at surface. One is comparing the experimental spectra with few predicted ones, and select the one that most matches to the experimental one. Another one is running an exhaustive algorithm to explore the most possible solution space [7]. However, both approaches take a lot of time and computational resources. Therefore, applying LP will result a large gain in computation.

The LP solver we use is called "GNU linear programming tool kit" (GLPK). It has implemented both simplex and interior point methods in C programming language. It is open-source and intended to solve large scale LP problems.

1.4 Conclusion and Open Questions from Previous Study

My research is based on Hung's study [4]. In his study, he mentioned that generating model spectra that match the target experimental spectra from a list of known candidates is a way to extract molecular orientation information at surface. The traditionally exhaustive way of achieving this goal consumes too much computational effort, therefore, he introduced LP approach to vibrational spectroscopy study. The LP approach results in pseudo polynomial time $O(n)$, which is a great improvement compared to $O(n!)$.

However, depends on different test case settings, the LP approach may not always return the target composition of candidates that generates the mock target experimental spectra. When considering the candidates from one type of molecule at surfaces, the return solution of the LP approach does not match the known target composition. When considering the candidates from a mixture of molecules, the return solution of the LP approach does match the know target composition. The reason why the LP approach failed to return the target composition has not been thoroughly studied by Hung.

Moreover, when applying the LP approach, only SFG spectral information has been considered in his LP model. The possibility and applicability of using IR and Raman spectral information to the LP approach have not been considered. Meanwhile, the possibility of combining different spectral information to the LP approach has not been considered neither.

1.5 Aims and Scope

The goal of my study is to figure out the underlying properties of the LP approach, figure out what is the cause that the LP approach fails to obtain the target composition of candidates in some test cases. Based on the gained information, I further explore the applicability of the LP approach to different test cases. My plan is applying the LP approach to a simplified molecular model first, so that only the properties

of our LP model can be focused.

With the properties learnt from the first step, the LP approach is then applied to realistic molecules. There are two types of test cases, one is considering the candidates coming from one type of realistic molecule, to see if the LP approach can return the target composition of the mock spectra. Another one is considering the candidates coming from different types of realistic molecules. If the LP approach achieve in obtaining the target composition, then how the LP approach applied systematically will be studied.

The purpose is to check if LP approach will return the target composition of the spectra for one type of molecule at surfaces. If yes, whether the LP model can be applied generally to one type molecule will be studied. If not, what is the underlie reason will be explored. Similar study will also be applied to different molecules at surfaces. At last, the experimental spectral information is brought into consideration.

1.6 Overview of the Thesis

Chapter 1 briefly introduces the aim and scope of the current study. Chapter 2 explains the current approaches to extract the molecular orientation distribution at surfaces, as well as how to produce IR, Raman and SFG spectra. Chapter 3 aims to use a simplified molecular model to study the properties of our LP model. Chapter 4 applies our LP approach to one type of molecule at surfaces. Chapter 5 applies the LP approach to a mixture of different molecules at surfaces. Chapter 6 applies the LP approach to experimental spectral data. Chapter 7 is the conclusion and future work.

Chapter 2

Methods

2.1 Description

Before analyzing the LP model and applying it to the realistic molecules' vibrational spectra, there are a few factors to address. First of all, creating each amino acid's IR, Raman and SFG spectra is an essential step. This part of research has been done thoroughly by Hung [4]. In this chapter, I introduce the content that is related to my study.

2.2 Structure of Realistic Molecules

Figure 2.1 illustrates the molecule structure of the six amino acids in the molecular frame.

2.3 Generating Model Spectra

To generate these amino acids' vibrational spectra, a molecule's vibration modes need to be modelled in the molecular frame, then transferred to the laboratory frame to work with the systems where surfaces exist. Chapter 2 in Hung's thesis [4] describes how to perform electronic structure calculations using GAMESS [6] to obtain the derivatives of every dipole moment and polarizability. Then he introduced how to use Direction Cosine Matrix (DCM) to transfer these two derivatives from the molecular frame to the laboratory one. After that, Euler angles could be extracted from

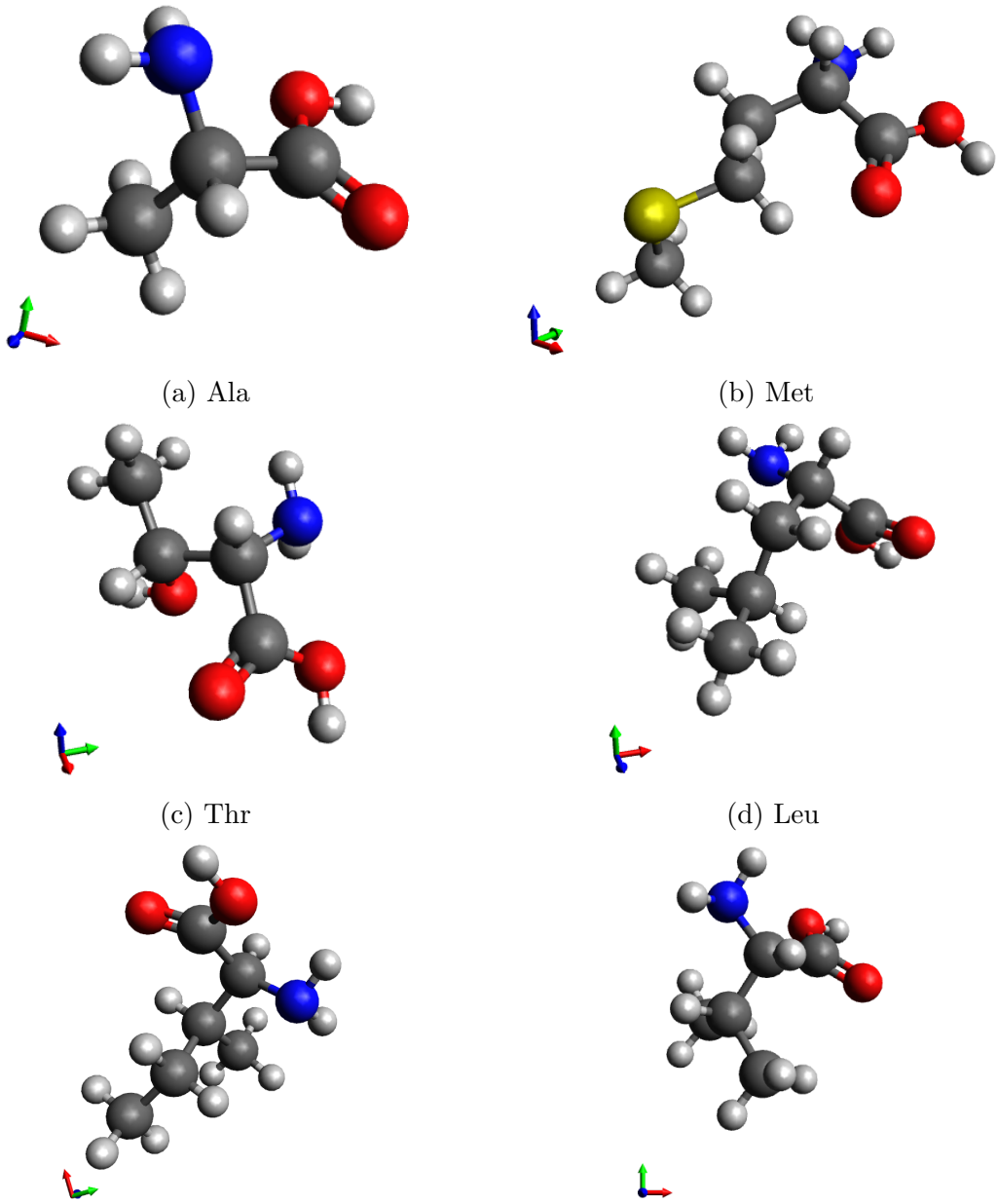

(a) Ala (b) Met

(c) Thr (d) Leu

(e) Ile (f) Val

Figure 2.1: Molecule structure of Ala, Met, Thr, Leu, Ile and Val in molecular frame. Blue axis is designated as z axis, red axis is designated as a axis, green is designated as b axis.

DCM. Euler angles are used to describe a molecule's orientation at surfaces. They are labelled by θ, ϕ and ψ as shown in Figure 2.2. They are referred as *tilt*, *azimuthal* and *twist* angles, respectively. Let x, y and z be lab frame Cartesian coordinates, and a, b and c be the molecular frame coordinates. *Tilt* angle θ is the angle between z and c. *Azimuthal* angle φ is the rotation about z. *Twist* angle ψ is a twist about c [7]. After three steps of successive rotations of Euler angles, molecule properties can be transferred from the molecular frame to the lab one.

In order to achieve the above steps, Hung first did a Hessian calculation using GAMESS. Secondly, 7 snapshots of a molecule vibrating in different modes were taken. Thirdly, he did a force field calculation to obtain the derivatives of dipole moment and polarizability for each 7 snapshot moment. Then the derivatives of dipole moment and polarizability are obtained by the interpolation of these 7 snapshot moment. Because the two obtained derivatives are in the molecular frame, Hung used DCM to convert these two derivatives into the lab frame. Then abstracted Euler angles from DCM. After these electronic structure calculations, the derivatives information, which is the molecular property information, is obtained.

In my study, those molecular property information is used to generate the amino acids' spectral information directly. Each molecule's property information contains the derivatives of dipole moment and polarizabilities of each vibrational mode. Depends on the number N of atoms in a molecule, there are $3N - 6$ vibrational modes. Furthermore, Equation 2.2 to 2.5 are used to generate the amino acids' IR, Raman and SFG spectra.

All the test cases in my study are limited to only consider the *tilt* angle distribution of Euler angles, and assume isotropy on *twist* and *azimuthal* angular distributions. A uniform distribution is applied to *twist* and *azimuthal* angles. For angle φ, it requires the surfaces to be not striped. There can be no anisotropy in the plane of the surface. Because of this, we can limit the candidate number by integrating angle φ. For angle ψ, a uniform distribution implies that a molecule has cylindrical symmetry in its preference of surface. The molecule can be tilted, but has no '*twist*' preference. With the integration of these two Euler angles, the number of candidates for one molecule will be greatly reduced. Therefore, a candidate in my study is a specific molecule with specific θ value. However, the number of the candidates is still

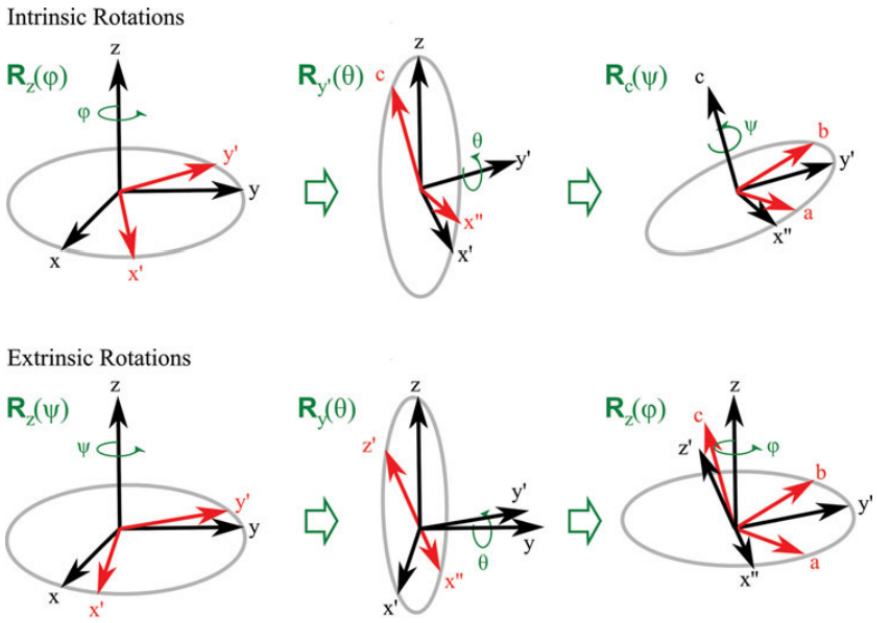

Figure 2.2: The Euler angles represented as the spherical polar angles θ, φ and ψ, and the illustration of the three successive rotations that transform the lab x, y, z coordinate system into the molecular a, b, c frame intrinsically and extrinsically. Reproduced from Ref. 7.

large when only considering θ angle. For example, when every 10° a candidate is obtained, there are 18 candidates of one molecule. In the mixture of six molecules, the number of possible combinations of all these molecules' candidates is $18^6 = 34012224$.

When molecules lay on a surface, the orientation of each single molecule varies. To simulate the vibrational spectra, a reasonable orientation distribution for the molecules needed to be studied. The orientation distribution requires either do a molecular dynamic simulation to study the distribution of molecule orientations at surface, or come up with an analytic orientation distribution function. In my study, the LP model is appropriate for the second method is selected. Moreover, δ-distribution function shown in Equation 2.1 is used to represent the molecule orientation distribution that models the spectrum signals. This means that all the molecules are tilted at one same angle at surface. This assumption is applied across the whole study.

$$f_{(\theta)} = \delta(\theta - \theta_o) \tag{2.1}$$

The absorption of a (IR) spectrum is proportional to the square of the lab-frame dipole moment derivative. For example, the x-polarized absorption spectrum is given by Equation 2.2:

$$A_x(\omega_{\mathrm{IR}}) = \sum_q \frac{1}{2m_q\omega_{\mathrm{q}}} \left\langle \left[\frac{\partial u_x}{\partial Q}\right]_q^2 \right\rangle \frac{\Gamma_q^2}{(\omega_{\mathrm{IR}} - \omega_{\mathrm{q}})^2 + \Gamma_q^2} \tag{2.2}$$

where A_x represents x-polarized IR obsorbance. The same equation applies to A_y and A_z. ω_{IR} is the frequency of the probe radiation, μ is the dipole moment, m_q is the reduced mass, w_q is resonance frequency. Γ_q is the homogeneous line width, is set to 6 in all the test cases. Q_q is the normal mode coordinate of the qth vibrational mode. All values of ω_{IR}, μ, m_q, Q are obtained from the electronic structure calculations. Furthermore, because ϕ and ψ angles are integrated, the x-polarized spectrum is identical with the y-polarized one. Therefore, there are only two unique polarized IR spectra. For simplicity, IR spectra are referred as x and z in future test cases.

The intensity of Raman scattering is proportional to the square of lab frame transition polarizability. For example, Raman spectroscopy with an x-polarized excitation source collects the x-polarized component of the scattered radiation, which can be approximated by Equation 2.3.

$$I_{xx}(\Delta\omega) = \sum_q \frac{1}{2m_q\omega_{\mathrm{q}}} \left\langle \left[\frac{\partial \alpha_{xx}^{(1)}}{\partial Q}\right]_q^2 \right\rangle \frac{\Gamma_q^2}{(\Delta\omega - \omega_{\mathrm{q}})^2 + \Gamma_q^2} \tag{2.3}$$

where I_{xx} represents xx-polarized Raman intensity. Δw is the Stokes Raman shift. $\alpha_{xx}^{(1)}$ is one component of the 9-element polarizability tensor. m_q, w_q, Γ_q, and Q_q are the same as defined above for IR spectra. All the values of ω_{IR}, μ, m_q, Q are obtained from the electronic structure calculations. Similar to IR spectroscopy, because of the integration of ϕ and ψ angles, only 4 unique spectra are obtained from the following polarization: xx, xy, xz and zz. For simplicity, Raman spectra are referred as xx, xy, xz and zz in future test cases.

SFG spectral signal is the imaginary part of the second-order susceptibility, $\left|\chi^{(2)}\right|$. $\chi^{(2)}$ is derived from the second-order polarizability $\alpha^{(2)}$ as shown in Equation 2.4.

The imaginary part of $\left|\chi^{(2)}\right|$, which is SFG spectral signal, is displayed as Equation 2.5.

$$\chi^{(2)}_{xxz}(\omega_{\mathrm{IR}}) = \sum_{q} \frac{1}{2m_q\omega_{\mathrm{q}}} \left\langle \left[\frac{\partial\alpha^{(1)}_{xx}}{\partial Q}\right]_q \left[\frac{\partial u_z}{\partial Q}\right]_q \right\rangle \frac{1}{\omega_{\mathrm{q}} - \omega_{\mathrm{IR}} + i\Gamma_q} \tag{2.4}$$

$$\mathrm{Im}\left[\chi^{(2)}_{\mathrm{xxz}}(\omega_{\mathrm{IR}})\right] = \sum_{\mathrm{q}} \frac{1}{2\mathrm{m_q}\omega_{\mathrm{q}}} \left\langle \left[\frac{\partial\alpha^{(1)}_{\mathrm{xx}}}{\partial \mathrm{Q}}\right]_{\mathrm{q}} \left[\frac{\partial \mathrm{u_z}}{\partial \mathrm{Q}}\right]_{\mathrm{q}} \right\rangle \frac{\Gamma_{\mathrm{q}}}{(\omega_{\mathrm{q}} - \omega_{\mathrm{IR}})^2 + \Gamma^2_{\mathrm{q}}} \tag{2.5}$$

where $\chi^{(2)}_{xxz}$ is the second-order susceptibility. It is probed by an x-polarized visible incoming beam at frequency ω_{vis} and a z-polarized infrared beam incoming with frequency ω_{IR}. Both incoming beams are incident to the sample. Then the x-component at frequency $\omega_{\mathrm{SFG}} = \omega_{\mathrm{vis}} + \omega_{\mathrm{IR}}$ is selected for detection. As $i = \sqrt{-1}$ is in the denominator, $\chi^{(2)}$ is a complex value [4]. The SFG response considered in this thesis is the imaginary component of the $\chi^{(2)}$. Same as IR and Raman spectroscopy, all the values of ω_{IR}, μ, m_q, Q are obtained from the electronic structure calculations. Because of the integration of ϕ and ψ angles, only 3 unique non-zero spectra are obtained from the following polarizations: xxz, xzx and zzz. For simplicity, SFG spectra are referred as xxz, xzx and zzz in future test cases.

With these equations and the electronic structure calculations, IR, Raman and SFG spectra can be generated for a candidate of a molecule. Taking Methionine as an example, Figure 2.3 displays x-polarized IR spectra of the following candidates: Methionine with θ equals 0°, 20°, 40° and 60°. Their spectra are prefixed with *candidate_* in the labels. *ir_x_* indicates the spectroscopy technique, "number" indicates the θ angle's value. The spectra labelled as *target_ir_x*, is generated by combining 10% of *candidate_ir_x_*0, 50% *candidate_ir_x_*20 and 40% *candidate_ir_x_*40.

Similarly, Figure 2.4, 2.5 and 2.6 depict the spectra of the same candidates and targets for z-polarized IR, xx-polarized Raman and xxz-polarized SFG spectrum respectively. In Figure 2.3, the biggest differences among the candidates exist at each vibrational mode. The valid range for the wavenumber is from 1000 to 2000.

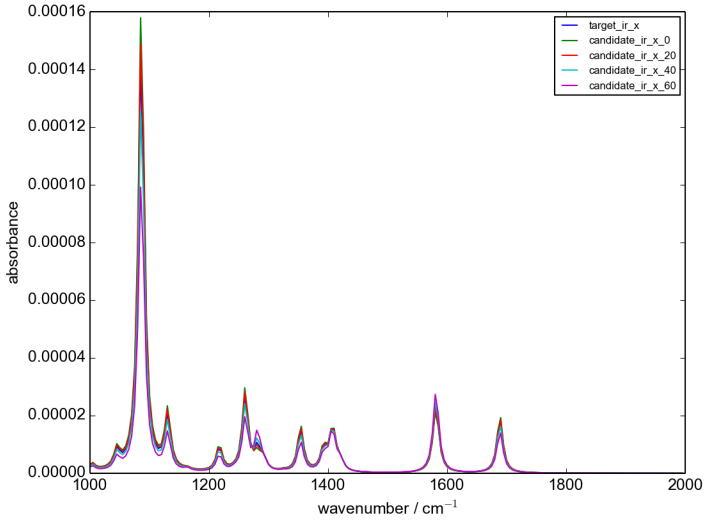

Figure 2.3: IR x-polarized spectra of methionine's four candidates and target. The candidates are with θ of 0°, 20°, 40° and 60°. The target is produced by combining 10% of *candidate_ir_x_0*, 50% *candidate_ir_x_20* and 40% *candidate_ir_x_40*.

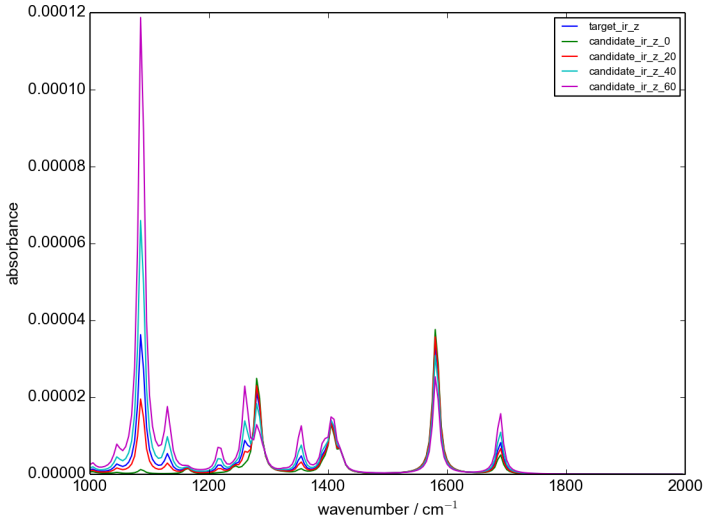

Figure 2.4: IR z-polarized spectra of methionine's four candidates and target. The candidates are with θ of 0°, 20°, 40° and 60°. The target is produced by combining 10% of *candidate_ir_x_0*, 50% *candidate_ir_x_20* and 40% *candidate_ir_x_40*.

2.4 Conclusion

Chapter 2 briefly explains what are the current approaches to extract molecular orientation distribution at surfaces, the molecular structures of six amino acids, and how

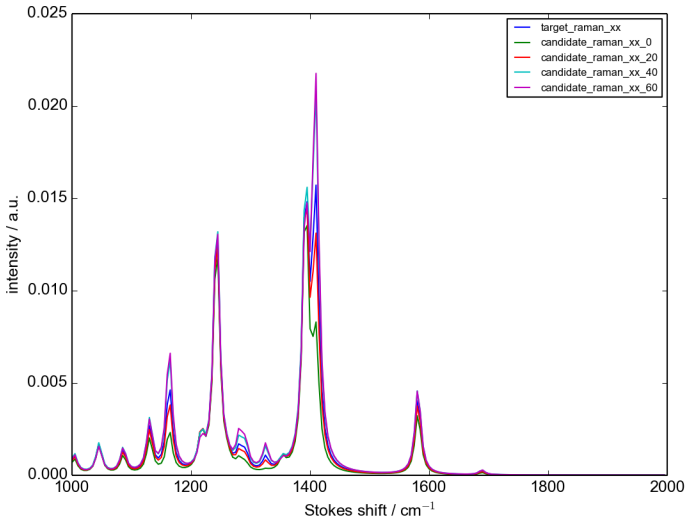

Figure 2.5: Raman xx-polarized spectra of methionine's four candidates and target. The candidates are with θ of 0°, 20°, 40° and 60°. The target is produced by combining 10% of *candidate_ir_x_0*, 50% *candidate_ir_x_20* and 40% *candidate_ir_x_40*.

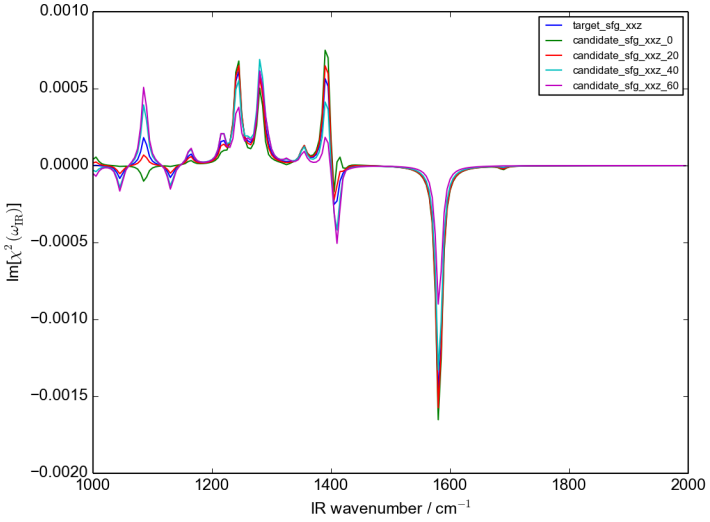

Figure 2.6: SFG xxz-polarized spectra of methionine's four candidates and target. The candidates are with θ of 0°, 20°, 40° and 60°. The target is produced by combining 10% of *candidate_ir_x_0*, 50% *candidate_ir_x_20* and 40% *candidate_ir_x_40*.

to produce IR, Raman and SFG spectra theoretically. In Chapter 3, the properties of the LP model are studied. It is conducted by using a simplified molecular model to gain an insight of the behaviours our LP approach. The motivation of creating a

simplified molecular model is to create a molecule as simple as possible, so that only the properties of the LP model is focused. With the further information gained in Chapter 3, further test cases will be run for realistic molecules in Chapter 4, 5 and 6.

Chapter 3

Simplified Molecular Model

3.1 Description

The goal of Chapter 3 is to introduce the formulas used to describe our LP model. As well as exploring the properties of the LP model by using a simplified molecular model. The purpose of introducing the simplified molecular model is to limit the complexity that comes from the parameters needed to describe the realistic models, so that the analysis of the nature of the LP model can be focused. Our goal is to figure out with the spectral information available, could our LP model extract any valuable information.

The simplified molecular model contains 4 vibration modes. Theses vibrational peaks are at frequencies of 2850, 2960, 3050 and 3200 cm^{-1}. The widths of the peaks are 5, 10, 5 and 15 cm^{-1}, respectively. The amplitudes of the peak are 1, 0.7, -0.2 and 0.5 cm^{-1}, respectively. The comparing angles of the peaks are $15°, 90°, 0°$ and $60°$.

Only IR spectroscopy is considered for the simplified molecule. Equation 3.1 is used to generate the z-polarized IR spectrum. Moreover, both ϕ and ψ Euler angles are integrated, only the difference on angle θ is considered.

$$f_\theta(\omega_{\text{IR}}) = \sum_{q=1}^{4} A_q^2 cos^2(\theta - \theta_q) \frac{\Gamma^2}{(\omega_{\text{IR}} - \omega_{\text{q}})^2 + \Gamma^2} \tag{3.1}$$

where A_q is the amplitude, θ_q is the comparing angle, Γ is the width, and ω_{q} is the frequency. Ten candidates are produced with 10 different θ values as follows: 0°, 10°, 20°, 30°, 40°, 50°, 60°, 70°, 80°, 90°. Their spectra are shown in Figure 3.1. The 10 candidates have peaks at the same frequencies. The spectral signal for candidates is comparatively strong at each peak.

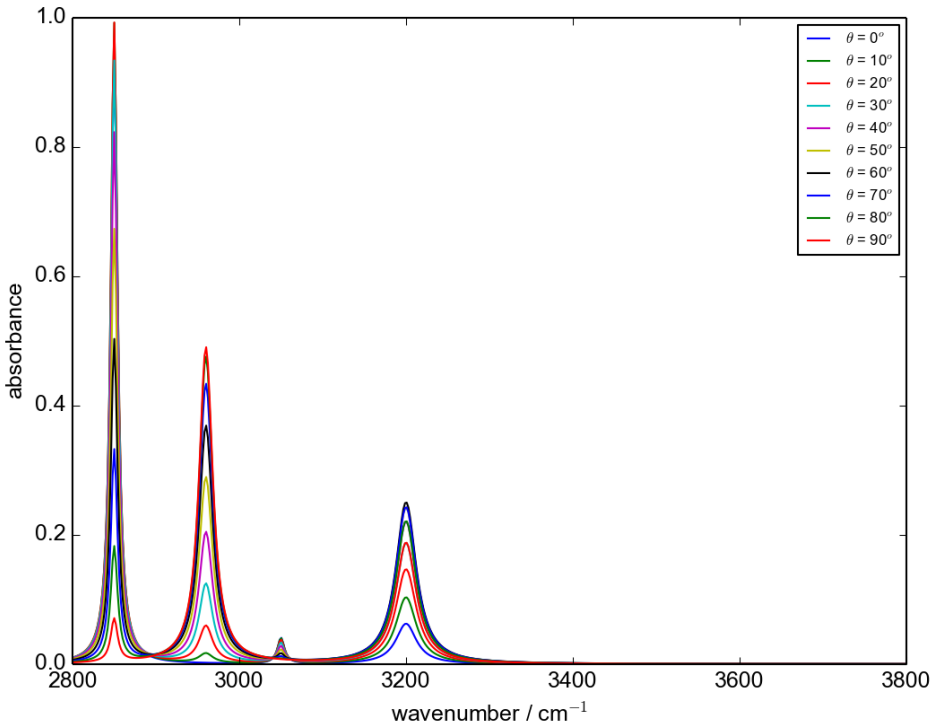

Figure 3.1: z-polarized IR spectra of candidates of simplified molecular model

3.2 Linear Programming Model for Spectral Study

Equation 3.2 is used to construct the LP model. The optimal solution returned by the LP solver is then compared with the target composition to see if they match each other. This equation has also been used to study the composition of Ribonucleic acid (RNA) with ultraviolet (UV) spectra [8] and other UV spectroscopy studies [9] back in the 60s.

$$\underset{p_c}{\text{minimize}} \sum_{n=1}^{N_p} \left| \text{Target} - \sum_{\text{c}=1}^{\text{N}_\text{c}} \text{p}_\text{c} \text{f}_\theta(\text{x}) \right| \tag{3.2}$$

where p_c are the unknown percentages of the candidate, which are the decision variables. These percentages are returned by LP solver, and called return composition in future test cases. N_p is the number of points selected along the wavenumber, both for candidates and target spectra. Target refers to the corresponding data points selected in target spectra. N_c is the number of candidates. For each data point, the absolute residual between the target spectrum and the one composed by the decision variables is calculated. The objective function minimizes the sum of the absolute residuals over all the data points.

However, because of the absolute signs in the objective function, Equation 3.2 is not an LP problem. Transforming the absolute signs is needed in order to use LP approach. It is achieved by introducing one more variable X and two more constraints to each data point as shown in Equation 3.3. The previous model in Equation 3.2 is then converted into the one in Equation 3.4, and it can be solved by an LP solver. At last, one more constraint is introduced to restrict the sum of the percentages to be 1.

$$\begin{aligned} X &= \left| \text{Target} - \sum_{\text{c}=1}^{\text{N}_\text{p}} \text{p}_\text{c} \text{f}_\theta(\text{x}) \right| \\ X &\geq \text{Target} - \sum_{\text{c}=1}^{\text{N}_\text{c}} \text{p}_\text{c} \text{f}_\theta(\text{x}) \\ X &\geq -\text{Target} + \sum_{\text{c}=1}^{\text{N}_\text{c}} \text{p}_\text{c} \text{f}_\theta(\text{x}) \end{aligned} \tag{3.3}$$

$$
\begin{aligned}
&minimize \sum_{n=1}^{N_p} X_p \\
&\mathrm{X_1} - \mathrm{Target_1} + \sum_{\mathrm{c}=1}^{\mathrm{N_c}} \mathrm{p_c f_\theta(x_1)} \geq 0 \\
&\mathrm{X_1} + \mathrm{Target_1} - \sum_{\mathrm{c}=1}^{\mathrm{N_c}} \mathrm{p_c f_\theta(x_1)} \geq 0 \\
&\vdots \\
&\mathrm{X_n} - \mathrm{Target_n} + \sum_{\mathrm{c}=1}^{\mathrm{N_c}} \mathrm{p_c f_\theta(x_n)} \geq 0 \\
&\mathrm{X_n} + \mathrm{Target_n} - \sum_{\mathrm{c}=1}^{\mathrm{N_c}} \mathrm{p_c f_\theta(x_n)} \geq 0 \\
&\sum_{c=1}^{N_c} p_c = 1
\end{aligned} \tag{3.4}
$$

Note that the LP model exactly describes our problem to be solved. Assuming that we can obtain sufficiently precise data, solving the LP will yield the target composition. Recall if the solution space is feasible and bounded, then there is a unique optimum solution.

3.3 Linear Programming Model Implementation

Next, I describe how to solve Equation 3.4 by implementing our LP model. Code is written to generate a file that contains all the candidates' spectral information needed for the test cases. In this step, the molecular property information that generated from the electronic structure calculations are used. For a specific candidate, given the molecular property information and a θ value, the candidate's spectral information is obtained. To further illustrate, a candidate class is written. This class defines how to use the molecular property information to generate the needed spectral information. Given a candidate's molecular property information and a θ value, a instance of this specific candidate is created. For the simplified molecule, this class only contains IR spectral information.

In the second step, more code is written to generate a target composition of a list of candidates. Then the target composition is used to generate the target spectra. The probe range, which is the range of the wavenumber, is from 2800 to 3300 cm^{-1} for the simplified molecule. It is from 2000 to 3000 cm^{-1} wavenumber for realistic molecules. The target spectral information is generated in the same text file as candidate's spectral information. Depend on the test case setting, code can be used to generate text files that contain selected types of spectral information.

In the third step, the LP model is constructed by using the spectral information text file generated in the second step. This part of the code was written by Hung [4]. It reads all the candidates and target spectral information, and builds the LP model as shown in Equation 3.4, then output it to an LP input file.

In the fourth step, we use LP solver "GNU linear progarmming tool kit" (GLPK) to read the LP input file, then obtain the result composition.

3.4 Test Cases

In Case 1 and 2, 4 candidates are selected, the detailed setting is shown in Table 3.1. In Case 1, there are 4 candidates with θ of $0°, 10°, 20°$, and $30°$. In Case 2, the four candidates are with θ values of $0°, 5°, 10°$, and $15°$. Instead of having a 10 degree variance in θ, 5 degree difference is applied on θ in Case 2. This means that when the candidates become more similar to each other than the ones in Case 1 as their spectra are more similar. In both cases, 100 data points are selected evenly along the wavenumber from z-polarized IR spectra. The target composition of the candidates are the same for both cases. In Case 1, the return composition is the same as the target one, however, the return composition for Case 2 does not match the target one.

In order to figure out why the return composition in Case 2 is different from the target one, the spectra generated by the return composition is plotted together with the target spectra as shown in Figure 3.2. Note that the result spectra is identical to the target one. The residual between them is 0. In order to see whether this observation is a general case, Case 3 is set up in Table 3.2. Case 3 contains more candidates

Test Case index	1	2
Number of Candidates	4	4
Candidates	[0, 10, 20, 30]	[0, 5, 10, 15]
Target Composition	[0.1, 0.5, 0.4, 0]	[0.1, 0.5, 0.4, 0]
Number of Data Points	100, z	100, z
Return Composition	[0.1, 0.5, 0.4, 0]	[0, 0.80, 0.10, 0.1]

Table 3.1: Test case 1 and 2 setting using simplified molecular model

than Cases 1 and 2. 10 candidates are included with θ values ranging from 0° to 90°.

Table 3.2 indicates the return composition of Case 3 is different from the target one. Figure 3.3 shows that the spectrum produced by the return composition is almost identical to the one generated by the target composition in Case 3. The residual is negligible as well. This observation is the same as Case 2.

Among Case 1, 2 and 3, only the return composition of Case 1 matches its target one. However, in Case 2, the difference in θ value among the candidates is smaller than Case 1. In Case 3, the number of the candidates is larger than Case 1. Both effects increase the complexity of the test cases. In both Case 2 and 3, the spectrum constructed by the return composition matches to the one built by the target composition.

The above observation demonstrates that there are multiple compositions can achieve in constructing the spectrum that are close to the target one. The numerical limitation helps the LP solver to converge to a unique optimum solution. The reason for Case 1 to return a composition that matches to the target one, is that the spectral information applied to the LP model is competent. The constraints constructed in the LP model for Case 1 eventually converge to the target composition.

In order to add necessary information to construct the constraints in our LP model, IR's second polarization is introduced to the simplified molecule: the x polarization. Figure 3.4 describes how the x-polarized spectra presented for 10 candidates. Case

Test Case index	3
Number of Candidates	10
Candidates	[0, 10, 20, 30, 40, 50, 60, 70, 80, 90]
Target Composition	[0.1, 0, 0.5, 0, 0.4, 0, 0, 0, 0, 0]
Number of Data Points	100, z
Return Composition	[0, 0, 0.73, 0, 0.21,0, 0, 0.057, 0, 0]

Table 3.2: Test case 3 setting of simplified molecule

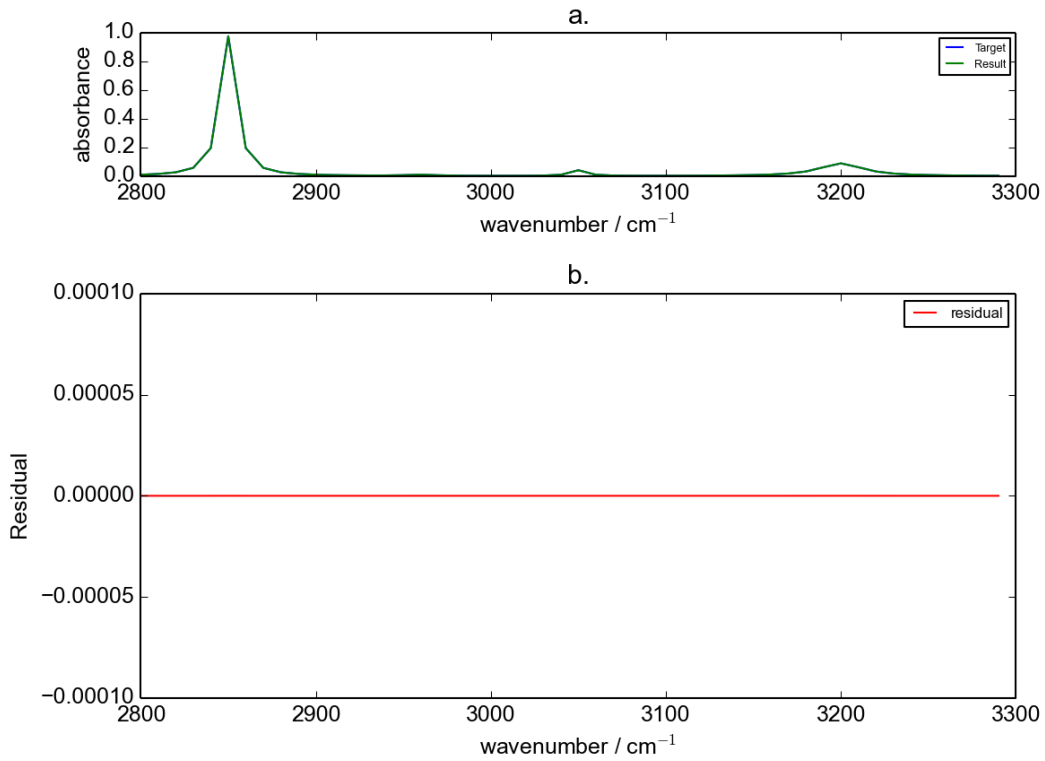

Figure 3.2: a. z-polarized IR target spectrum plotted with the one constructed by the return composition in Case 2 of simplified molecular model; b. the residual plot between the spectra.

4 and 5 include both polarizations' spectral information in the LP model. In Table 3.3, Case 4's setting is based on Case 2, with x-polarized IR spectral information added. 100 data points are selected from this additional spectrum, then converted to additional decision variables and constraints in the LP model. Case 5 is based on Case 3, with x-polarized IR spectral information added. In both Case 4 and 5, the return composition matches to the target one. This further proves that as long as we have sufficing information for the LP model, the LP solver returns a composition matches to the target one.

3.5 Constraint Study Based on Test Case 4

From Case 1 to 5 of simplified molecule, we know having sufficient information in our LP model is the key to obtain the target composition. Having sufficient information

Test Case index	4	5
Number of Candidates	4	10
Candidates	[0, 5, 10, 15]	[0, 10, 20, 30, 40, 50, 60, 70, 80, 90]
Target Composition	[0.1, 0.5, 0.4, 0]	[0.1, 0, 0.5, 0, 0.4, 0, 0, 0, 0, 0]
Number of Data Points	100, z 100, x	100, z 100, x
Return Composition	[0.1, 0.5, 0.4, 0]	[0.1, 0, 0.5, 0, 0.4, 0, 0, 0, 0, 0]

Table 3.3: Test case 4 and 5 setting of simplified molecule

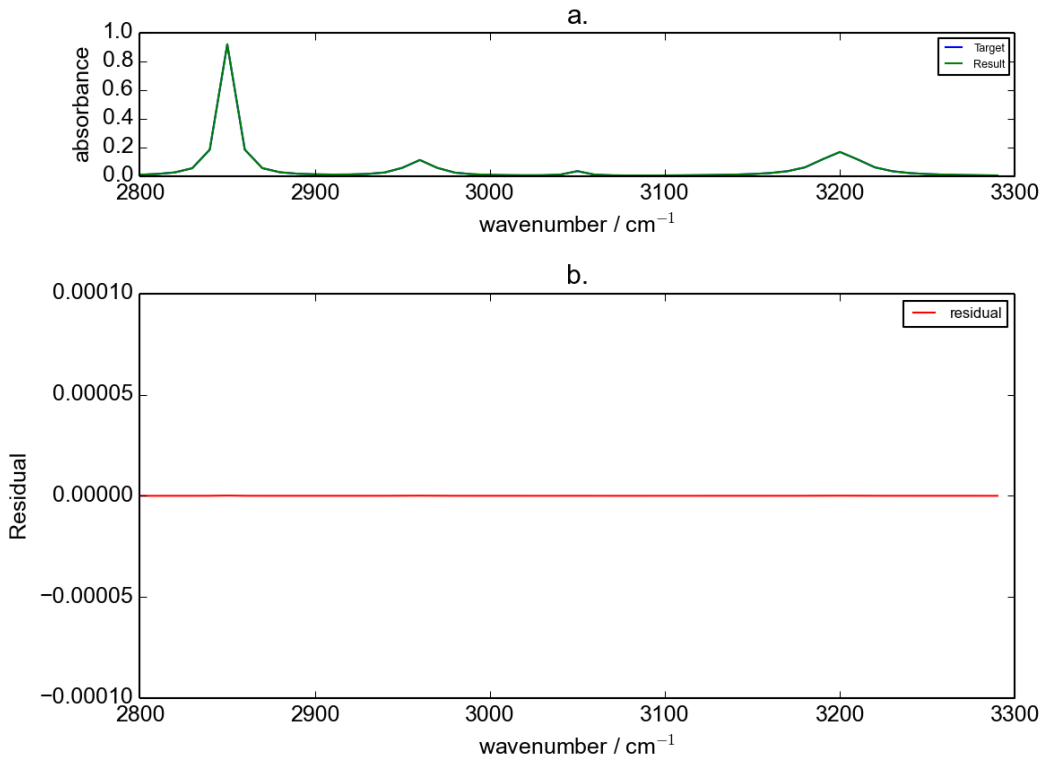

Figure 3.3: a. z-polarized IR target spectrum plotted with the one constructed by the return composition in Case 3 of simplified molecular model; b. the residual plot between the two spectra

means having enough constraints to help to converge to the desired target composition. The information is coming from the data points selected along the spectra. This leads us to do a more detailed study on the constraints in order to see how many data points are enough to get the target composition.

Based on Case 4, test cases about applying different data information to the LP model are conducted in Table 3.4. The number of data points indicates how many data points are selected. Points Selection shows how data points are selected. For example, [2800, 3300, 50] means along wavenumber from 2500 to 3300, every 50 wavenumber a data point is selected along a spectrum. z and x indicate the corresponding polarization of IR spectrum.

As Table 3.4 indicates, the return compositions of Case 6 to 14 are the same. To the contrary, from Case 15, the return composition matches the target one. In Figure

Test Case #	# Data Points	Points Selection	Return Composition
6	10	[2800, 3300, 50], z	[0, 0.8, 0.10, 0.1]
7	20	[2800, 3300, 25], z	[0, 0.8, 0.10, 0.1
8	25	[2800, 3300, 20], z	[0, 0.8, 0.10, 0.1]
9	32	[2800, 3300, 15], z	[0, 0.8, 0.10, 0.1]
10	50	[2800, 3300, 10], z	[0, 0.8, 0.10, 0.1]
11	100	[2800, 3300, 5], z	[0, 0.8, 0.10, 0.1]
12	$100 + 1$	[2800, 3300, 5], z [2800, 3300, 500], x	[0, 0.8, 0.10, 0.1]
13	$100 + 5$	[2800, 3300, 20], z [2800, 3300, 100], x	[0, 0.8, 0.10, 0.1]
14	$100 + 10$	[2800, 3300, 20], z [2800, 3300, 50], x	[0, 0.8, 0.10, 0.1]
15	$100 + 50$	[2800, 3300, 20], z [2800, 3300, 10], x	[0.1, 0.5, 0.4, 0]
16	$100 + 100$	[2800, 3300, 20], z [2800, 3300, 5], x	[0.1, 0.5, 0.4, 0]

Table 3.4: Constraint study based on Case 4 of simplified molecular model. For more precise result data, refer Table A.3.

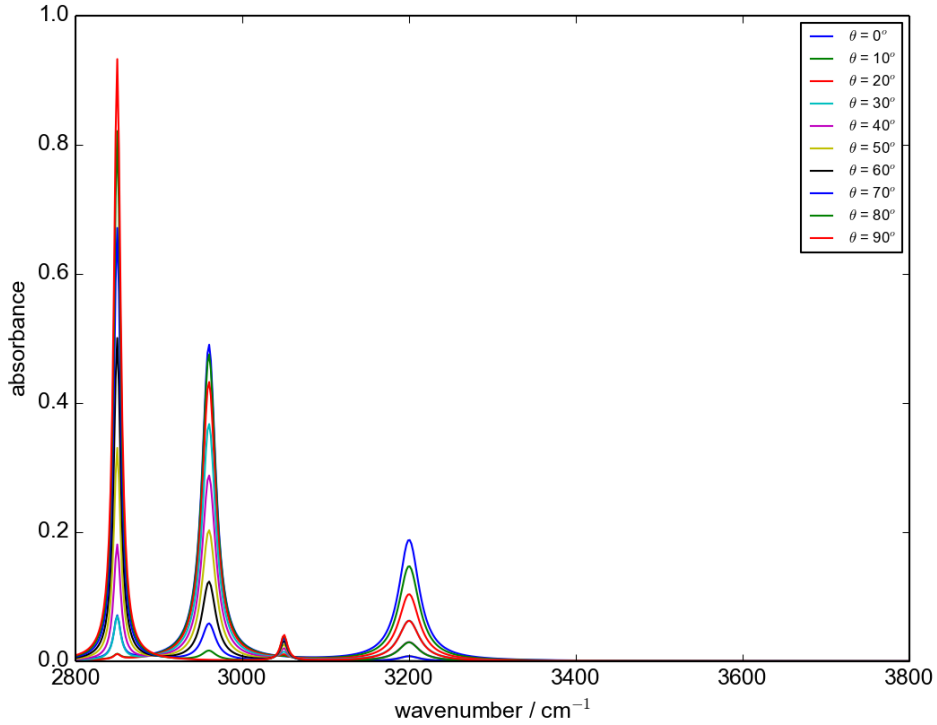

Figure 3.4: x-polaried IR spectra of candidates of simplified molecular model with θ value expanded from 0° to 90°

3.5 displays the spectra conducted by $[0, 0.80, 0.1, 0.1]$ and $[0.1, 0.5, 0.4, 0]$, both x- and z-polarized IR spectra generated by these two compositions are identical.

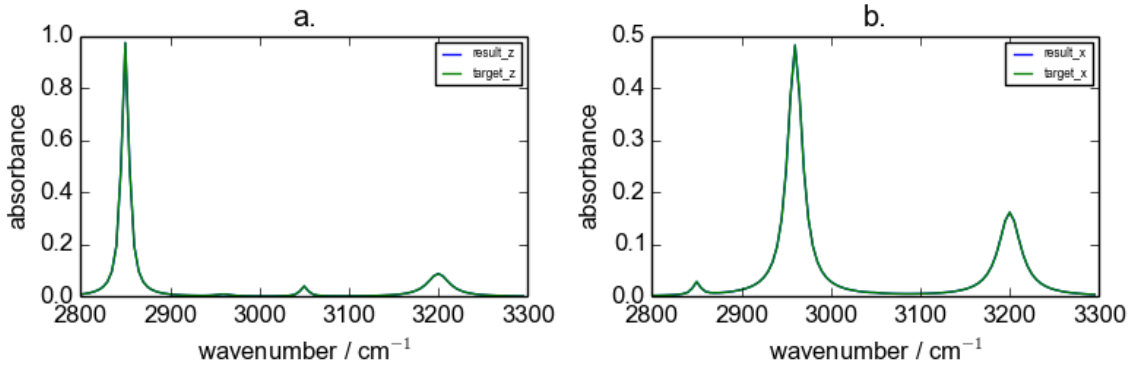

Figure 3.5: IR spectra plotted by the return compositions from the constraint study based on Case 4 of simplified molecule. a. z-polarized IR spectra; b. x-polarized IR spectra.

3.6 Constraint Study Based on Test Case 5

Based on Case 5, similar constraint study is conducted as displayed in Table 3.5, and the same observation is obtained as the test cases in Table 3.4. When the result composition $[0, 0, 0.73, 0, 0.21, 0, 0, 0.057, 0, 0]$ and target one are used to plot the spectra, the produced spectra are almost identical as shown in Figure 3.6. Although these two constraint studies do not give a clear answer about how many data points are enough to get the target composition, it confirms that as long as the spectral information is sufficient, the LP solver will return the target composition.

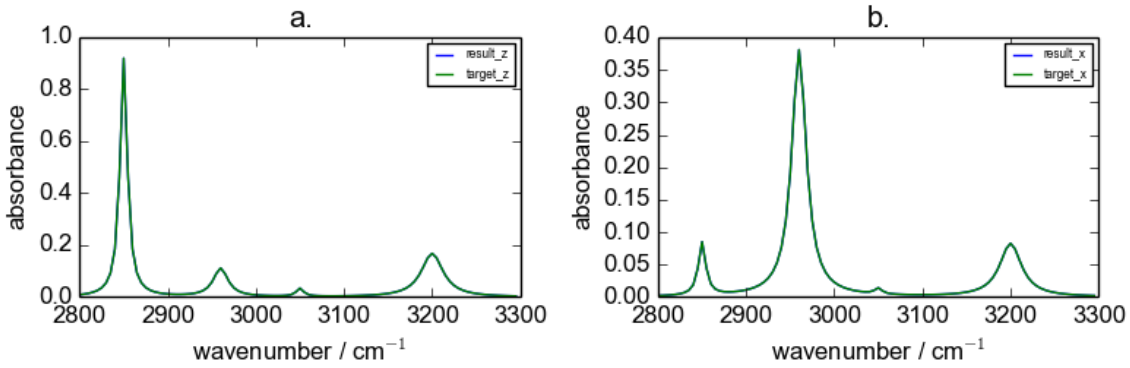

Figure 3.6: IR spectra plotted by the return compositions from the constraint study based on Case 5 of simplified molecular model. a. z-polarized IR spectra; b. x-polarized IR spectra.

3.7 Discussion and Conclusion

Recall that our LP model, for the right data set is expected to return the target composition. We can conclude that, if the target composition is not returned correctly, then the data we collect is not sufficient to describe the test cases to the LP model.

However, when the target composition is not returned correctly, the return composition does build spectra that are identical to the target ones. This means that there are more than one composition can build the spectra that are identical to the target ones. Because of the numerical limitation, an unique optimum solution of the LP model is always obtained.

Test Case #	# of Data Points	Point Selection	Return Composition
17	10	[2800, 3300, 50], z	[0.16, 0, 0, 0.83, 0, 0, 0, 0, 0, 0.017]
18	25	[2800, 3300, 20], z	[0, 0, 0.73, 0, 0.21, 0, 0, 0.057, 0, 0, 0]
19	50	[2800, 3300, 10], z	[0, 0, 0.73, 0, 0.21, 0, 0, 0.057, 0, 0, 0]
20	100	[2800, 3300, 5], z	[0, 0, 0.73, 0, 0.21, 0, 0, 0.057, 0, 0, 0]
21	500	[2800, 3300, 1], z	[0, 0, 0.73, 0, 0.21, 0, 0, 0.057, 0, 0, 0]
22	$100 + 1$	[2800, 3300, 5], z [2800, 3300, 500], x	[0, 0, 0.73, 0, 0.21, 0, 0, 0.057, 0, 0, 0]
23	$100 + 10$	[2800, 3300, 5], z [2800, 3300, 50], x	[0.36, 0, 0.31, 0.33, 0, 0, 0, 0, 0]
24	$100 + 20$	[2800, 3300, 5], z [2800, 3300, 25], x	[0.17, 0, 0, 0.79, 0, 0, 0.035, 0, 0, 0]
25	$100 + 25$	[2800, 3300, 20], z [2800, 3300, 20], x	[0.17, 0, 0, 0.79, 0, 0, 0.035, 0, 0, 0]
26	$100 + 50$	[2800, 3300, 5], z [2800, 3300, 10], x	[0, 0, 0.75, 0, 0.15, 0, 0.1, 0, 0, 0]
27	$100 + 84$	[2800, 3300, 5], z [2800, 3300, 6], x	[0.17, 0, 0, 0.79, 0, 0, 0.035, 0, 0, 0]
28	$100 + 100$	[2800, 3300, 5], z [2800, 3300, 5], x	[0.1, 0, 0.5, 0, 0.4, 0, 0, 0, 0, 0]

Table 3.5: Constraint study based on Case 5 of simplified molecular model. For more precise result data, refer Table A.4.

With the help of the simplified molecular model, we know the reason why the LP model cannot return the target composition all the time. In the next step, I want to figure out with all the spectral information available for a realistic molecular model, can the LP model return the target composition?

Chapter 4

Realistic Molecular Model

4.1 Description

After experimenting with the simplified molecular model, lacking sufficient spectral information is the key cause for the failure of obtaining the target composition. First of all, in the simplified molecular model, there are only four vibrational modes, the spectral information is limited. Secondly, the similarity among the candidates is high, as all the candidates are coming from one same molecule. Third, only IR spectra is considered.

In this chapter, test cases are conducted using realistic molecules. In addition to IR, both Raman and SFG spectra are calculated for these molecules, which makes the study one step closer to the overall goal and scope. The realistic molecule focused on this chapter is Met amino acid.

Same as the simplified molecular model, in order to limit the possible candidate space of Met, *twist* and *azimuthal* angular distributions are assumed to be isotropic, which are integrated. Only θ in Euler angles is considered in Met's surface orientation distribution function. In Chapter 2 section Generating model spectra, I have explained how a molecule's IR, Raman and SFG spectra are generated. Two unique IR spectra can be obtained from x, and z polarizations. Four unique Raman spectra can be obtained from xx, xy, xz and zz polarizations. Three unique SFG spectra can be obtained from xxz, xzx and zzz polarizations.

Test Case #	1	2
# Candidates	4	4
Candidates	[0, 20, 40, 60]	[0, 20, 40, 60]
Target Composition	[0.1, 0.5, 0.4, 0]	[0.1, 0.5, 0.4, 0]
# Data Points	200 x	200 z
Return Composition	[0.70, 0, 0, 0.30]	[0.70, 0, 0, 0.30]

Table 4.1: Test Case 1 and 2 setting for Met candidates

Test Case #	3	4
# Candidates	4	4
Candidates	[0, 20, 40, 60]	[0, 20, 40, 60]
Target Composition	[0.1, 0.5, 0.4, 0]	[0.1, 0.5, 0.4, 0]
# Data Points	200 x 200 z	200 x 200 xx
Return Composition	[0.70, 0, 0, 0.30]	[0.1, 0.5, 0.4, 0]

Table 4.2: Test Case 3 and 4 setting for Met candidates

The goal is to see if those spectral information is sufficient for the LP model to return the correct target composition of the candidates of one type molecule at interfaces. If yes, we need to figure out which spectral information is needed for the LP model. If no, we need to check if the cause of the failure is the same as the simplified molecular model.

4.2 Test Cases

In Table 4.1 and 4.2, four test cases are set up with four candidates and same target composition. These four candidates have θ of the following degree: 0°, 20°, 40° and 60°. The only difference among these four test cases is the spectroscopy information we select to apply to the LP model, and it is indicated by the Number of Data Points. In Case 1, only x-polarized IR spectral information is used. This means that only data points from x-polarized IR are selected to apply to the LP model. Same for Case 2, data points are obtained from spectra of IR's z-polarized IR. In Test Case 3, the spectral information of x and z-polarized IR are combined. At last, in Case 4, spectral information of x-polarized IR and xx-polarized Raman are combined. Case

4 contains the most abundant information, as its return composition matches to the target one.

When merely using IR information, the return composition is the same for Case 1, 2 and 3. Figure 4.1 displays the resulting spectra generated by using the return composition obtained from the first three test cases. The resulting spectra is almost identical to the target ones. It indicates that with only IR spectral information is not sufficient to get the target composition. However, the spectra built by the return composition matches the target spectra. This means that further information is needed to build the constraints of the LP model. The more constraints are introduced, the more accurate the return composition will be.

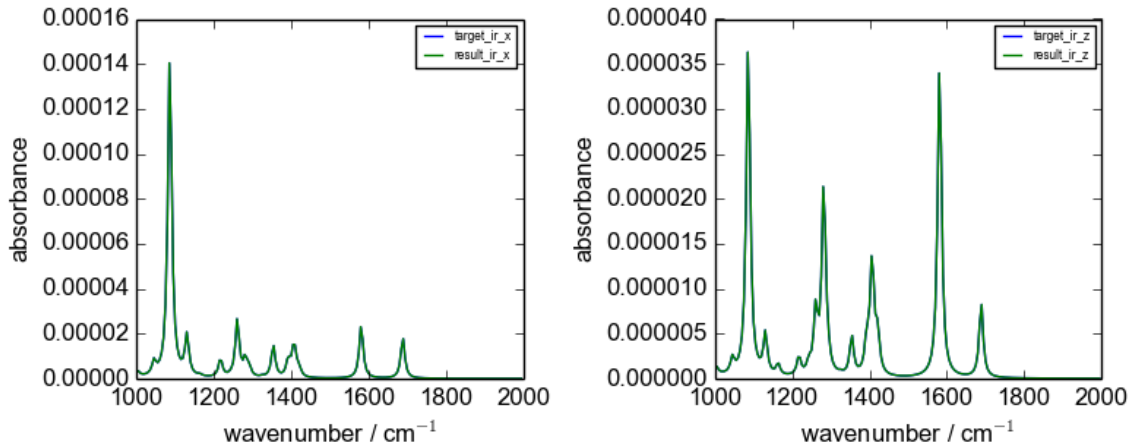

Figure 4.1: Compare target IR spectra with the ones generated by the return composition of Case 1, 2 and 3

In Case 4, combining IR and Raman spectral information is sufficient to obtain the target composition. When the difference in θ degree for candidates decreases from 20° to 10°. Checking if Raman and IR together is still sufficient to derive the target composition is desired. Therefore, the following test cases are conducted as shown in Table 4.3.

Case 5 shows that the LP model constructed by merely using IR spectral information is not sufficient to derive the target composition. Case 6 indicates that combining IR and Raman spectral information helps to derive the target composition. What's

# Candidates	4	
Candidates	[0, 10, 20, 30]	
Target Composition	[0.1, 0.5, 0.4, 0]	
Test Case index	# Data Points	Result Composition
5	200 x 200 z	[0.75, 0, 0, 0.23]
6	200 x 200 z 200 xx	[0.1, 0.5, 0.4, 0]
7	200 xx 200 xy 200 xz	[0.1, 0.5, 0.4, 0]
8	200 xx 200 xy 200 zz	[0.1, 0.5, 0.4, 0]
9	200 xx 200 xy 200 xz 200 zz	[0.1, 0.5, 0.4, 0]

Table 4.3: Test case 5 to 9 setting for Met candidates

more, Case 7, 8 and 9, illustrate that Raman spectral information itself is sufficient to obtain the target composition as well.

For test case setting in Table 4.1, 4.2 and 4.3, combining IR and Raman spectral information to construct a LP model is sufficient enough to obtain the target composition. In order to study the limitation of the LP model, the complexity of the test case setting needed to be increased. Therefore, another group of test cases are designed as shown in Table 4.4. There are 5 candidates included in the test cases. Each candidate has θ with the following degree: 0°, 10°, 20°, 30° and 40°. The target composition is more complex than previous test cases, each candidate takes 20% in the mixture.

Case 10 applys only IR spectral information to the LP model, and the return composition does not match the target one. Case 11 uses only Raman spectral information, and the return composition does not match to the target neither. Same for Case 12 that uses only SFG spectral information. From Case 13, different kinds of spectral information are combined. In Case 13, IR and Raman spectral information is used to produce the LP model, still the return composition is different from the target one. Case 14 combines Raman and SFG, Case 15 uses IR and SFG, Case 16 cooperates all the three spectral information, however, none of them returns a composition that matches the target one.

The results of Case 10 to 16 indicate that even combining all the spectral information of IR, Raman and SFG, it is still not sufficient to attain the target composition for the test cases set up in Table 4.4. The spectral information we apply to the LP model is showing its limitation in these test cases. In order to confirm the reason causing the LP model to returning the target composition is because of insufficient information, further test cases are conducted in Table 4.5.

Number of Candidates	5	
Candidates	[0, 10, 20, 30, 40]	
Target Composition	[0.2, 0.2, 0.2, 0.2, 0.2]	
Test case index	Constraints	Result
10	200 x 200 z	[0.61, 0, 0, 0, 0.40]
11	200 xx 200 xy 200 xz 200 zz	[0.25, 0, 0.50, 0, 0.25]
12	200 xxz 200 xzx 200 zzz	[0.32, 0, 0.31, 0.16, 0.21]
13	200 x 200 z 200 xx 200 xy 200 xz 200 zz	[0.25, 0, 0.50, 0, 0.25]
14	200 xx 200 xy 200 xz 200 zz 200 xxz 200 xzx 200 zzz	[0.32, 0, 0.31, 0.16, 0.21]
15	200 x 200 z 200 xxz 200 xzx 200 zzz	[0.32, 0, 0.31, 0.16, 0.21]
16	200 x 200 z 200 xx 200 xy 200 xz 200 zz 200 xxz 200 xzx 200 zzz	[0.32, 0, 0.31, 0.16, 0.2]

Table 4.4: Test Case 10 to 16 setting for Met candidates. For more precise result data refer Table A.1.

4.3 Test Cases to Explain the Limitation of LP Model for Met Molecule

To further explore the reason that LP model reaches its limitation for the realistic molecule, Case 17 and 18 are conducted. To make the study case more general than Case 1 to 16, candidates' θ values are expanded from 0° to 80°. In total, there are 9 candidates. Because the SFG spectra for θ of 90° is a straight line, it is excluded from all the test cases related to realistic molecules. For target composition, five candidates are randomly selected to be presented. The difference between Case 17 and 18 is that different amount of data points are selected to build the LP model. From all three spectroscopy techniques' spectral information, every 5 wavenumber a data point is selected for Case 17. Every 500 wavenumber a data point is selected for Case 18. As a result, Case 17 and 18 each returns a different composition. Both compositions do not match to the target one.

However, in both Case 17 and 18, when the return composition is used to generate the IR, Raman and SFG spectra, then these spectra are plotted together with the spectra created by the target composition. All the spectra are almost identical for IR, Raman and SFG. Figure 4.2, 4.3 and 4.4 display the spectra plotted by using the return composition and the target one of Case 17. Every spectrum is almost identical to each other as shown in the figures. Same for Case 18 as shown in Figure 4.5, 4.6 and 4.7. These figures prove again that there are more than one composition that can perfectly construct the target spectra. The data information used to construct the LP model is not sufficient to converge to the return compostion exactly matches to the target one. This conclusion exactly fits the result obtained from the test cases we have done with the simplified molecular model.

4.4 Conclusion

With all the test cases I have run with Met, I figure out that even combine all the available spectral information to our LP model, it is not guaranteed the return composition from LP model matches the target one. The reason is the same as applying spectral information of the simplified molecular model to the LP model.

# Candidates	9	
Candidates	[0, 10, 20, 30, 40, 50, 60, 70, 80]	
Target Composition	[0.22, 0.29, 0.052, 0.083, 0.36, 0, 0, 0, 0]	
Test Case #	# of Data Points	Result Composition
17	each 5 wavenumber of IR, Raman and SFG spectra	[0.16, 0.39, 0.0, 0.099, 0.35, 0.0, 0.0, 0.0, 0.0]
18	each 500 wavenumber of IR, Raman and SFG spectra	[0.40, 0.0, 0.20, 0.036, 0.36, 0.0, 0.0, 0.0, 0.0]

Table 4.5: Test case 17 and 18 to explain the limitation of our LP model for Met molecule. For more precise result data refer Table A.2.

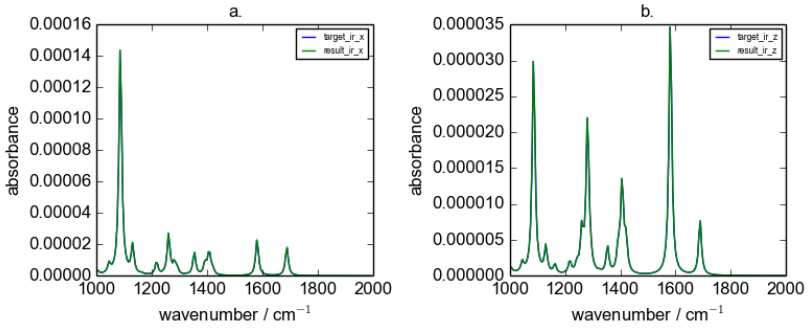

Figure 4.2: IR spectra plotted by using target composition and return composition of Case 17. a. x-polarized IR spectra; b. z-polarized IR spectra.

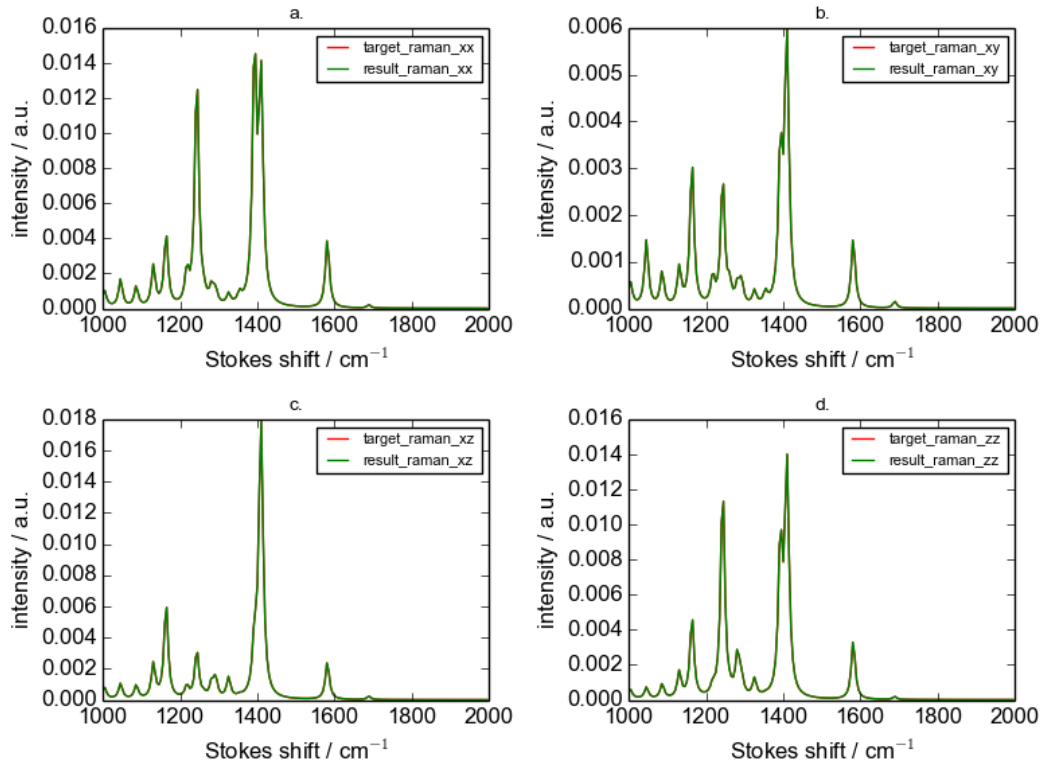

Figure 4.3: Raman spectra plotted by using the target composition and the return composition of Case 17. a. xx-polarized Raman spectra; b. xy-polarized Raman spectra; c. xz-polarized Raman spectra; b. zz-polarized Raman spectra.

The spectral information is not sufficient for the LP model in order to obtain the desired target composition. The spectra constructed by the return composition is identical to the target spectra.

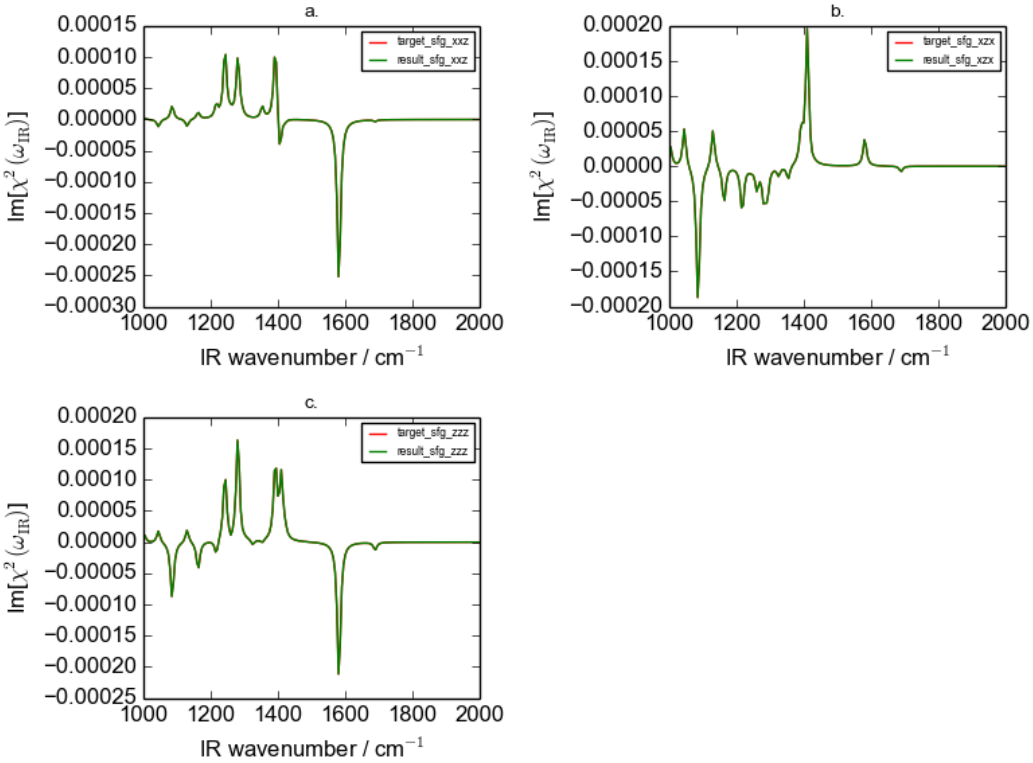

Figure 4.4: SFG spectra plotted by using the target composition and the return composition of Case 17. a. xxz-polarized SFG spectra; b. xzx-polarized SFG spectra; c. zzz-polarized SFG spectra.

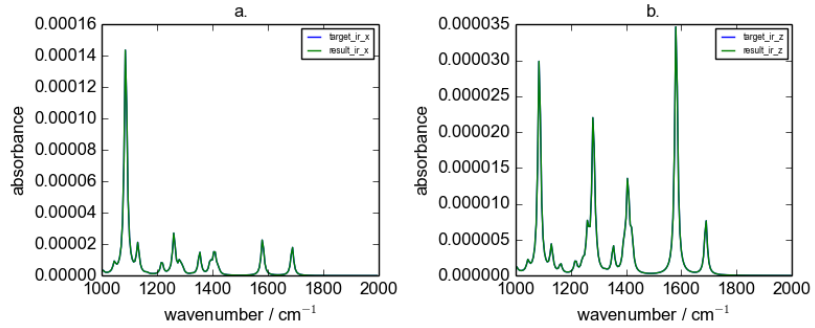

Figure 4.5: IR spectra plotted by using the target composition and the return composition of Case 18. a. x-polarized IR spectra; b. z-polarized IR spectra.

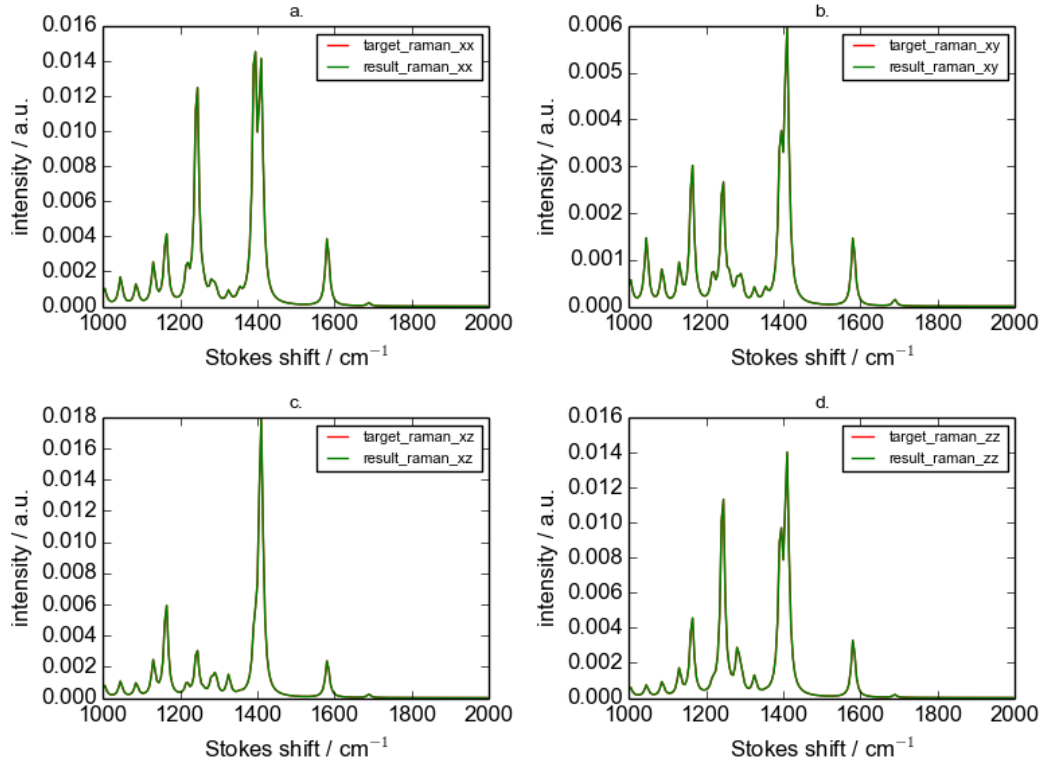

Figure 4.6: Raman spectra plotted by using the target composition and the return composition of Case 18. a. xx-polarized Raman spectra; b. xy-polarized Raman spectra; c. xz-polarized Raman spectra; b. zz-polarized Raman spectra.

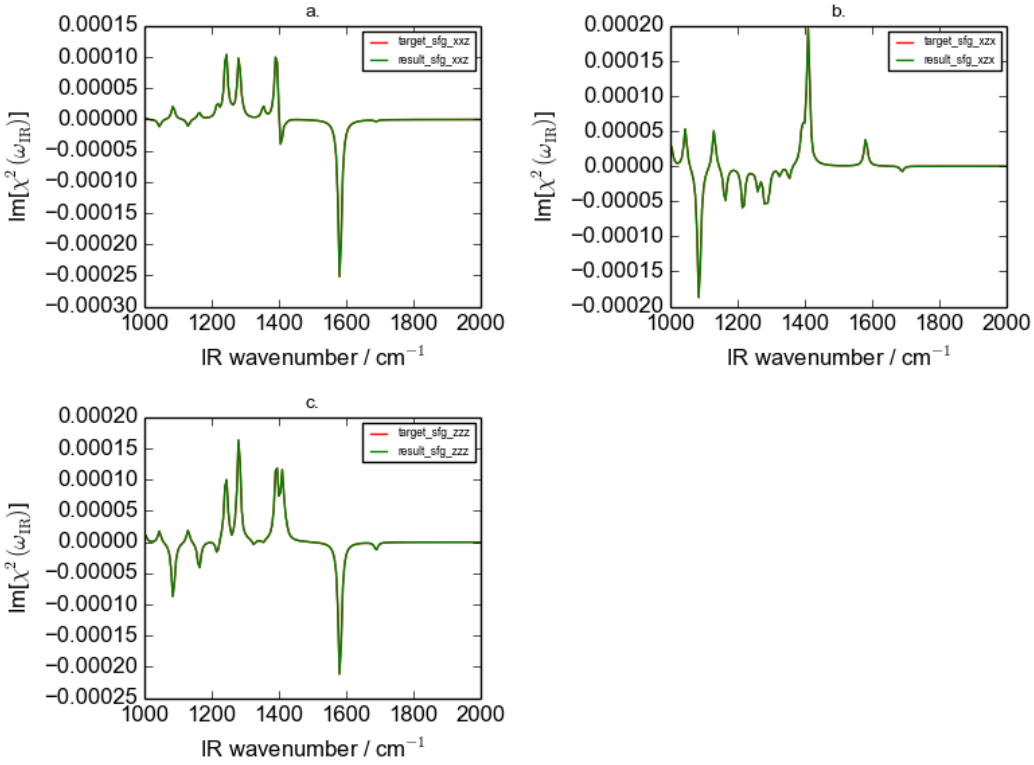

Figure 4.7: SFG spectra plotted by using the target composition and the return composition of Case 18. a. xxz-polarized SFG spectra; b. xzx-polarized SFG spectra; c. zzz-polarized SFG spectra.

Chapter 5

Mixture of Molecules

5.1 Description

In Chapter 4, test cases indicate that for one type of molecule at interfaces, even combining all the three spectral information, the constructed LP model cannot return the target composition in most cases. The existing spectral information is not adequate to obtain the target composition of one type of molecule at interfaces. Multiple return compositions can build the spectra that are almost exactly the same as the target ones. These compositions are returned by the LP models that use different amounts of spectral information. This indicates that even extracting data information from three spectroscopy techniques, it is still not sufficient to obtain the target composition for one type of molecule at interfaces. Besides one type of molecule at interfaces, we are also interested in the case where different molecules at interfaces. For a mixture of different molecules at interfaces, we want to figure out whether our LP model can help to obtain the target composition. If the LP model success in obtaining the target composition with certain spectral information, we want to know which spectral information. Moreover, we want to know the efficiency of the spectral information in obtaining the target composition.

5.2 Test Cases

5.2.1 Test Cases Considering Each Amino Acid Candidates from 0° to 80° on θ in the Mixture

To achieve the study of the orientation distribution of various molecules at interfaces, further test cases are constructed. These test cases have the following common settings.

First, there are six different amino-acids in the mixture: methionine, leucine, isoleucine(ile), alanine, threonine and valine. For each amino acid, only θ difference is considered, the other two Euler angles are integrated. Each amino acid molecule has 9 candidates in the mixture, they have θ of the following values: 0°, 10°, 20°, 30°, 40°, 50°, 60°, 70° and 80°. Because when θ equals 90°, the SFG spectra is a straight line. The corresponding candidate is excluded from all the test cases. As a result, there are 54 candidates in the mixture.

Second, the target composition need to be generated. The operation includes two steps: randomly pick one candidate from each amino acid's 9 candidates, then randomly generate a percentage for the selected candidate. The target composition is made of six randomly selected candidates with assigned percentage coming from the amino acids. The rest 48 candidates have 0 percentage in the target composition. Namely, six selected candidate makes 100% component of the mixture.

Third, the IR, Raman and SFG spectra need to be generated for all the 54 candidates and the target.

Table 5.1 displays a set of test cases, each test case contains different spectral information. In Case 1, candidates x- and z-polarized IR spectra are obtained. The target's IR spectra are generated by the dot product of the target composition and all the candidates' spectral data. Then the corresponding LP model is conducted using Equation 3.4. Therefore, we claim that the LP model in Case 1 only contains IR information.

Similarly, Case 2 contains only Raman spectral information of the following four

Test Case Index	Spectral Information
Case 1	x and z polarized IR spectra
Case 2	xx, xy, xz and zz polarized Raman spectra
Case 3	xxz, xzx and zzz polarized SFG spectra
Case 4	x and z polarized IR spectra xx, xy, xz and zz polarized Raman spectra
Case 5	x and z polarized IR spectra xxz, xzx and zzz polarized SFG spectra
Case 6	xx, xy, xz and zz polarized Raman spectra xxz, xzx and zzz polarized SFG spectra
Case 7	x and z polarized IR spectra xx, xy, xz and zz polarized Raman spectra xx, xzx and zzz polarized SFG spectra

Table 5.1: Detailed test cases set setting for the mixture of amino acids

polarizations: xx, xy, xz and zz. Case 3 contains only SFG spectral information of xxz, xzx and zzz three polarizations.

Starting from Case 4, spectral information of different spectroscopy techniques are combined. In Case 4, IR spectral information is combined with Raman. In Case 5, IR spectral information is combined with SFG. In Case 6, Raman and SFG spectral information are incorporated. At the end, in Case 7, all three spectral information are put together: IR, Raman and SFG.

Finally, this test case set is run 100 times in order to see which case in the set returns the target composition with the highest accuracy. This accuracy is measured by the time of each case returns the target composition. The scoring mechanism to measure whether a return composition matches to the target one is described in the next section.

5.2.2 Scoring method

At the first glance, the sum of residuals between the spectra composed by the return composition and the target one can be used to measure the accuracy of the return composition. However, in most test cases conducted earlier, the spectra generated by the return composition are almost identical to the ones created by the target composition. The sum of residuals between these spectra is negligible, which makes it appropriate to use as a scoring criteria.

Another way to measure the accuracy of the return composition, is to compare it directly with the target one. Calculating the sum of the residuals between a target composition and a return one directly can be a fast approach to evaluate the accuracy of each case. The shortage of this approach is that it cannot be used to measure in realistic test cases where the target composition is unknown. However, in the current test cases, this approach can be a way to evaluate the return composition for all the test cases where the target compositions are known in advance.

The return composition of each test case in the set is obtained for each run. Each return composition is compared with the target one to calculate the sum of the resid-

uals. If the sum is smaller than a certain threshold, which is 10^{-7}, then the return composition is considered to be the same as the target one.

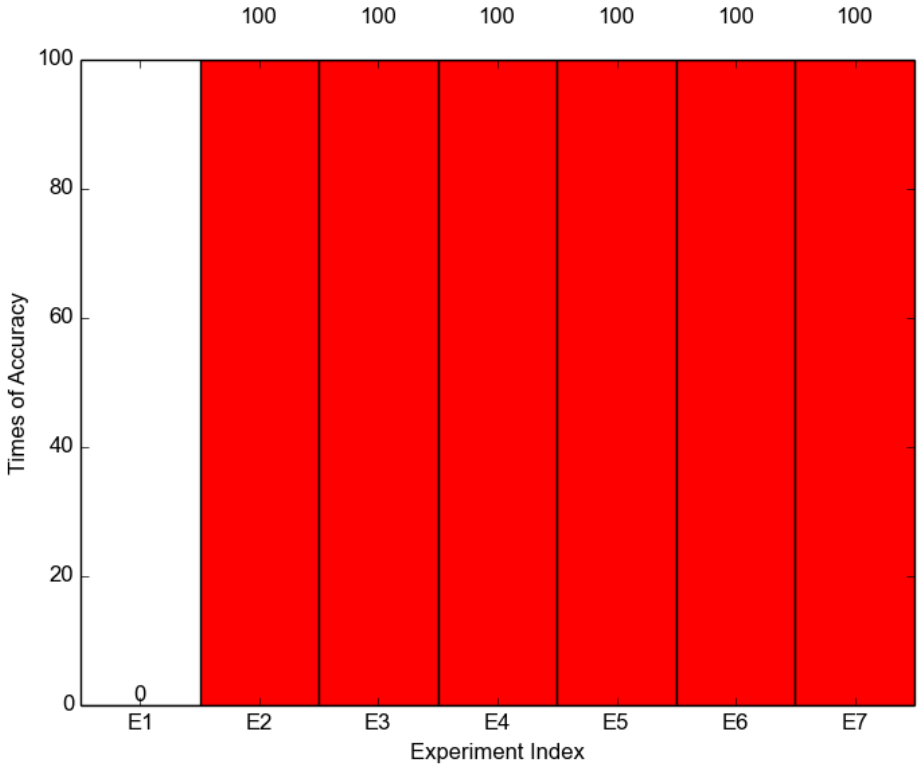

Figure 5.1: Accuracy analysis for test cases considering a mixture of amino acids with candidates from 0° to 80° on θ for each amino acid. Accuracy indicates how many times each test case in the set return a composition matches the target one.

The test case set is run 100 times based on the scoring method, the result is shown in Figure 5.1. Case 2, 3, 4, 5, 6 and 7, all return the target composition in the 100 runs. This result indicates that Raman or SFG alone is sufficient to obtain the target composition. For a mixture of amino acids with candidates from 0° to 80° on θ for each amino acid. Any test cases that contain Raman and SFG result in the same accuracy.

The only exception is Case 1. The accuracy is fairly low, which indicates that IR spectra do not contain sufficient information in order to obtain the target composition.

To take a further insight into the return composition of Case 1, the test case set is re-run 100 times, only the return composition of Case 1 is analyzed and focused. In

each run, IR x- and z-polarized spectra are plotted both by the returned composition and the target one. The result is that these spectra conducted by the two different compositions are very close to each other in each run. Randomly take one run as an example, Figure 5.2 displays the plotted spectra, and they are almost identical to each other. The residual is very small for the data points where these two spectra are not overlapped. This indicates that the optimum composition returned by the LP model conducted with only IR spectral information has achieved its best in obtaining a composition that best fit the target spectra.

(TODO: rewrite or remove this paragraph) Comparatively, SFG has three unique polarizations, and Raman has four unique polarizations. From each projection's spectrum, we evenly select 200 data points. This means that one more projection will bring in 200 more constraints or 400 more (when we take the absolute sign off) constraints to the LP model. This would make a huge difference in the LP model, in term of further refining the candidate selection in target composition. However, it is still too early for us to say that Raman has more orientation information because it has four unique polarizations. Because for Raman's any polarization, the spectrum of candidate with θ equals to one degree is identical to the one of candidate with this θ degree's complementary. For example, the Raman spectra for candidate with θ of 10°, is the same as candidate with θ of 170°. And for IR, it is the same case. Only SFG tells the differences between these two degrees, as the spectra for candidate with θ of one degree is symmetric to its complementary along wavenumber as shown in Figure **??**.

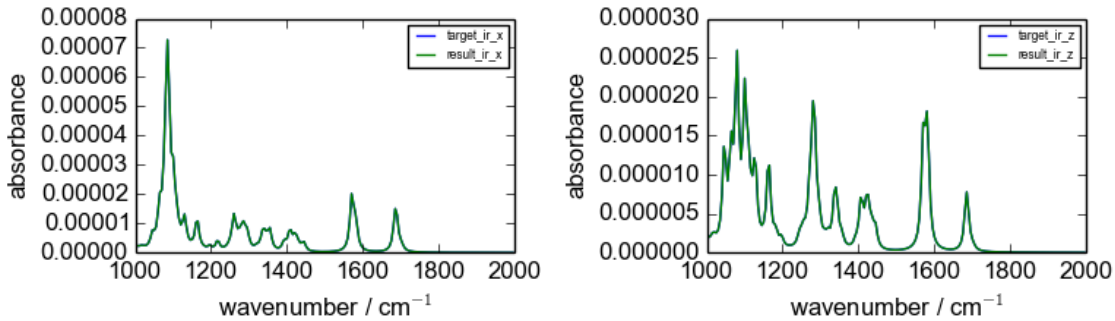

Figure 5.2: IR spectra plotted by the result composition and the target composition of one ramdon run when considering each amino acid candidates from 0° to 80° on θ in the Mixture.

5.2.3 Test Cases Considering Each Amino Acid Candidates from 0° to 180° on θ in the Mixture

To further study the capacity of the LP models built for the mixture of molecules,the candidate pool is expanded from 0° to 180° in terms of the θ value. Therefore, each amino acid has 18 candidates. In total, there are 108 candidates in the mixture. The same set of test cases in Table 5.1 is used. The only difference is instead of randomly select one candidate from 9 candidates, it is selected from 9. All 108 candidates' IR, Raman and SFG spectra need to be generated. Figure 5.3 illustrates the results obtained in 100 runs. The accuracy in Case 1 is still low. This is not surprising as the complexity of the candidates has increased. Moreover, IR spectra for candidate with θ of one degree is identical to the one with θ of this degree's complementary, as shown in Figure A.1. This also increases the difficulty for the LP model using IR spectral information to return the target composition.

However, it should be noticed that the accuracy for Case 2 has dramatically dropped. This can be caused by the Raman spectra for one candidate with a θ is identical to the one of this θ value's complementary as displayed in Figure A.2.

In Figure 5.3, the accuracy for Case 3 is no longer high neither. After increasing the number of amino acid candidates from 9 to 18, the complexity of the corresponding LP model has increased. Although the added candidates' SFG spectra are symmetric along wavenumber which may greatly increase the uniqueness of the candidates as shown in Figure A.3. The SFG spectral information is still insufficient to obtain the target composition.

The good result starts to emerge when using the combinations of IR and SFG or Raman and SFG. Figure 5.3 shows that Case 5, 6, and 7 all have 100% accuracies. This phenomenon can be explained as follow: SFG helps to distinguish a candidate from its complementary on θ value. The extra spectral information coming from IR or Raman helps to further refine the LP model, which can then converge the return composition to the target one.

Although the accuracy in Case 2 is low. There is still some noticable result in the return composition: for each amino acid, the percentage assigned is correct; however,

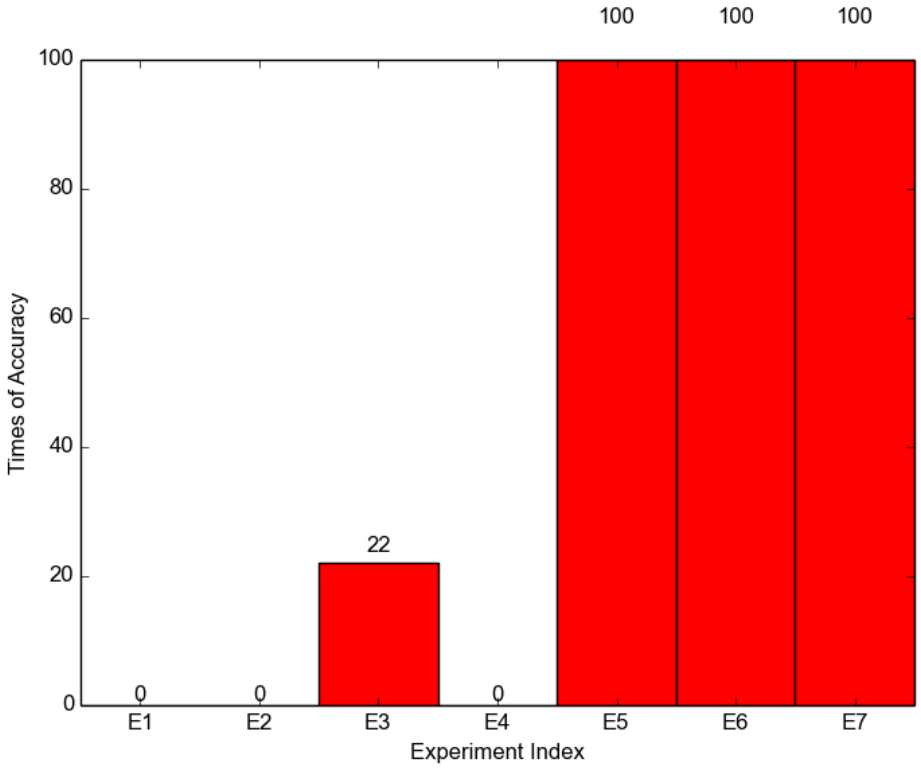

Figure 5.3: Accuracy analysis for test cases considering a mixture of amino acids with candidates from 0° to 180° on θ for each amino acid. Accuracy indicates how many times each test case in the set return a composition matches the target one.

the candidate presented may be always be correct. It is either the correct one, or the correct one's complementary. Randomly select one test case run as an example, Figure 5.4 displays the target composition. Figure 5.5 displays the return composition of Case 2 in the run. Figure 5.6 is the return composition of Case 6. Figure 5.4 and 5.6 are identical, which means the return composition of Case 6 is the same as the target one. The values in Figure 5.5 are the same as Figure 5.4. However, the position of each value is not the same in two the figures. For example, the percentage value 0.30 of methionine is for $\theta = 120°$ in Figure 5.4, but is for $theta = 60°$ in Figure 5.5. These two angles are complementary. This observation is the same for isoleucine, alanine, threonine, and valine in the figure. This observation is a general case across all the runs of the test case set. The return composition of Case 6 matches the target one. However, the return composition of Case 2 fails to pick each amino acid's correct candidate from this candidate's complementary. This can be explained as the Raman spectra for one θ are the same as its complementary.

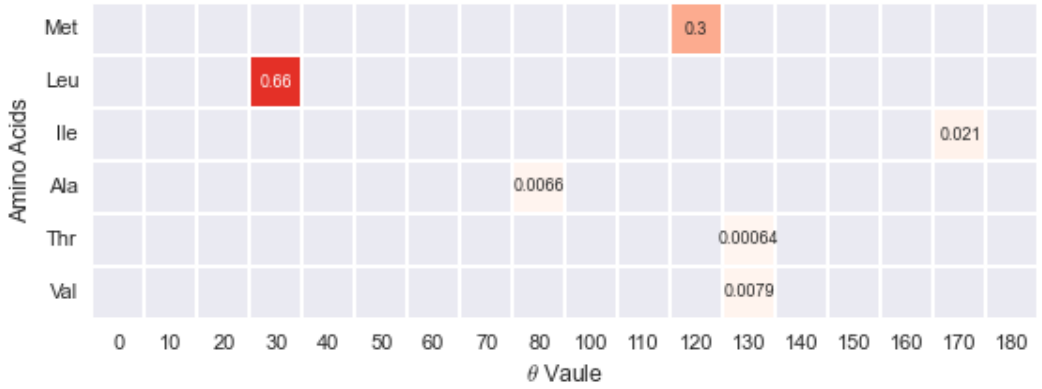

Figure 5.4: Target composition of one random run of six mixed amino acids with candidates expanded from 0° to 180° on θ for each amino acid. More detailed data of this target composition can be found in Appendix A.1.

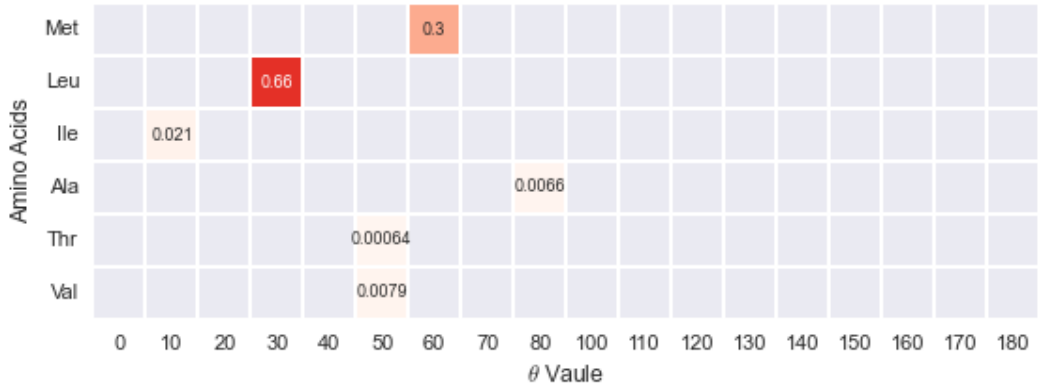

Figure 5.5: Return composition of Case 2 for one random run of six mixed amino acids with candidates expanded from 0° to 180° on θ. More detailed data of this return composition can be found in Appendix A.2.

The return composition of Case 4 is the same as the one of Case 2, which means combining IR spectra information with Raman is not sufficient for this test cases setting. This is because the IR spectra for one θ degree are also the same as its complementary. Spectral information from SFG is needed in order to study the cases that having θ expanded from 0° to 180°.

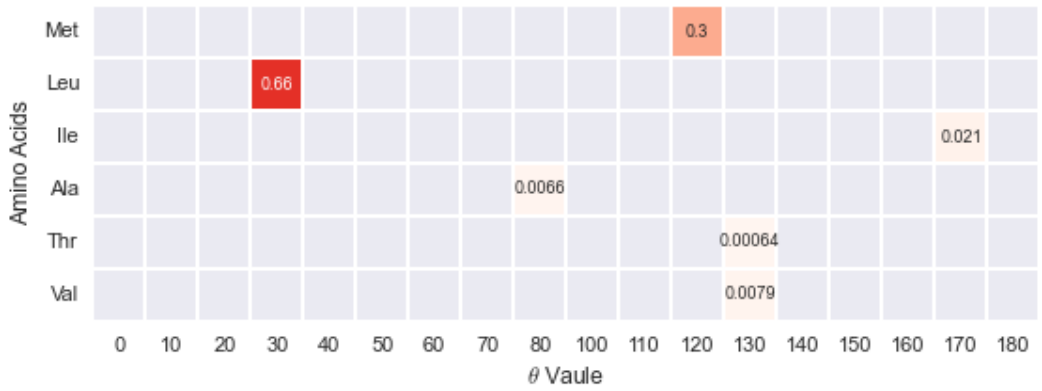

Figure 5.6: Return composition of Case 6 for one random run of six mixed amino acids with candidates expanded from 0° to 180° on θ. More detailed data of this return composition can be found in Appendix A.3.

5.3 Conclusion

Raman and SFG spectral information alone is sufficient to obtain the target composition, when considering a mixture of amino acids with candidates expanded from 0° to 80° on θ for each amino acid. When the candidates are expanded from 0° to 180° on θ, SFG spectral information needs to combine with IR or Raman in order to obtain the target composition.

Chapter 6

Possibilities for Treating Experimental Data

6.1 Description

The experimental spectra obtained from IR, Raman or SFG techniques have an amplitude scaling factor when compared to the candidate spectra generated mathematically. This means that between candidates' theoretical spectra and the experimental one, there is an unknown scaling factor. Within one particular spectroscopy technique, this scaling factor is the same for any polarization. Take IR as an example. The scaling factor for the spectrum of x polarization is the same as the one for the spectrum of z polarization. It is necessary to introduce this scaling factor to our LP model.

6.2 Test Case

6.2.1 Test cases with Scaling Factor Considering Each Amino Acid Candidates from 0° to 80° on θ in the Mixture

In Chapter 5, the LP model constructed by Cases 2 to 7 in Table 5.1 for θ ranged from 0° to 80° do well in retrieving the target composition for the mixed amino acids. Therefore, based on these test cases, we investigate the LP equations can be applied directly to the real experimental data for the same θ range.

Therefore, the same test case settings in Table 5.1 are used for the following test cases. The goal is the same, that is to figure out which spectral information helps to retrieve the target composition for the mixture of six amino acids' candidates. The only difference is that, in each run of the test case set, an arbitrary scaling factor is generated for IR, Raman and SFG, respectively. Therefore, the target spectra are not only composed by the target composition of all candidates, but also need to multiple by the randomly generated scaling factors of each spectroscopy technique.

To start with, we limit the scaling factors to be smaller than 1.

After a few runs of the test case set, it is observed that the returned compositions always contains one extra variable in every test case. For Case 2, 4, 6 and 7, the returned composition contains the correct selected candidates. However, the percentage values of the selected candidates are different from the target composition. The ratio between the returned percentage and the target percentage are the same for all the selected candidates. Furthermore, when this ratio adds up the extra variable, it equals 1. Randomly select one test case run as an example. Figure 6.2 displays the target composition, only the selected candidates are annotated with assigned percentage. Figure 6.2 displays the return composition of Case 2. The selected candidates in the return composition are correct. However, each percentage value is different from the one in the target composition. There is one extra value in Figure 6.2 with a value of 0.4.

Moreover, Equation 6.1 shows the ratio between the percentage of the selected candidates in the return composition and the target one is the same for all the amino acids (more precise calculated can be found in Appendix A.9). The value of this ratio is 0.6. When this ratio is added up with the extra variable (referred to as slack variable (SV) in LP) 0.4, the total is 1. As the scaling factors are pre-generated in the test case set, the value is known, which is 0.6 for Raman spectra. In conclusion, the SV is returned by LP. Then the scaling factor (SF) equals to $1 - SV$. From the scaling factor, the ratio between the return composition and the target one is known. At the end, the target composition can be re-built from the ratio and the return composition. The re-constructed target composition matches to the original one.

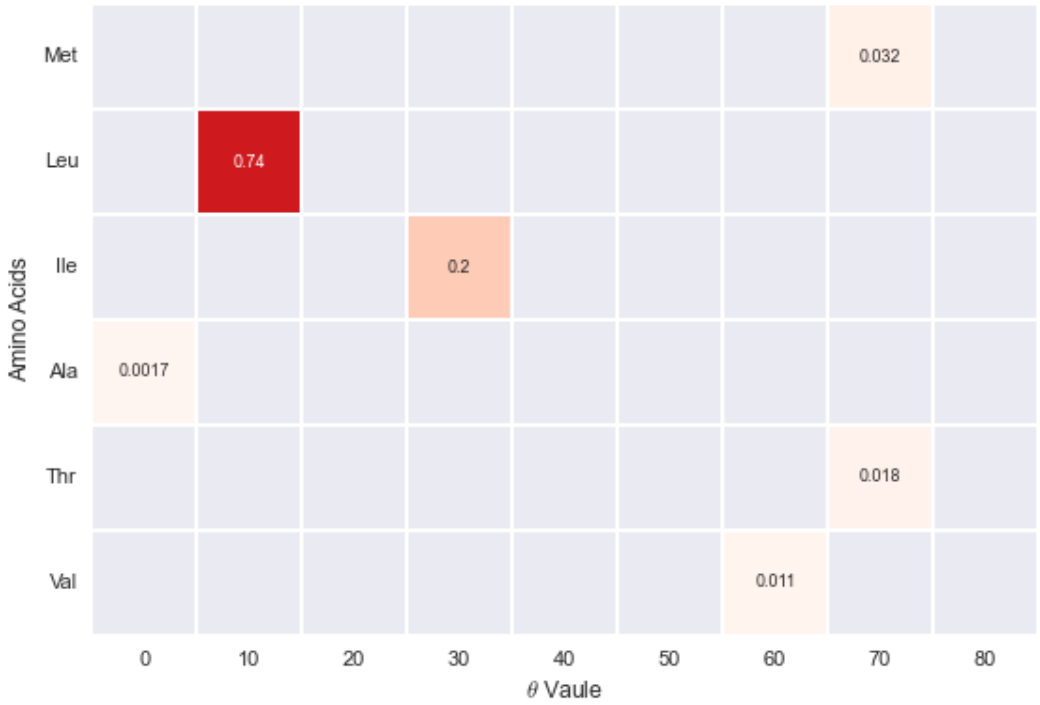

Figure 6.1: Target composition for one random run of the test case set with scaling factor for mixed amino acids, with θ expanded from 0° to 80°. More detailed data of this target composition can be found in Appendix A.4.

$$\frac{0.019}{0.032} = \frac{0.44}{0.74} = \frac{0.12}{0.2} = \frac{0.001}{0.0017} = \frac{0.011}{0.018} = \frac{0.0067}{0.011} = 0.6 \tag{6.1}$$

To varify if the above observation is a general case, the test case set in Table 5.1 is run 100 times with randomly generated scaling factors in each run. Figure 6.3 indicates the test case result. Case 2, 4, 6 and 7 hit the above observation with almost 100% frequency. This indicates that even with the scaling factor, Raman spectral information alone is sufficient to study the mixed molecules' orientation distribution at interfaces when each amino acid's candidates expanded from 0° to 80° on θ. The target composition can be re-constructed correctly from the return slack variable and the return composition. Figure 6.3 also illustrates that Case 3 does not hit the above observation with high frequency. With the scaling factor as the addition, SFG spectral information is not sufficient to obtain the target composition. Case 5 indicates that even combining IR and SFG spectral information, the constructed LP model cannot help to reconstruct the target composition. This can cause by the different

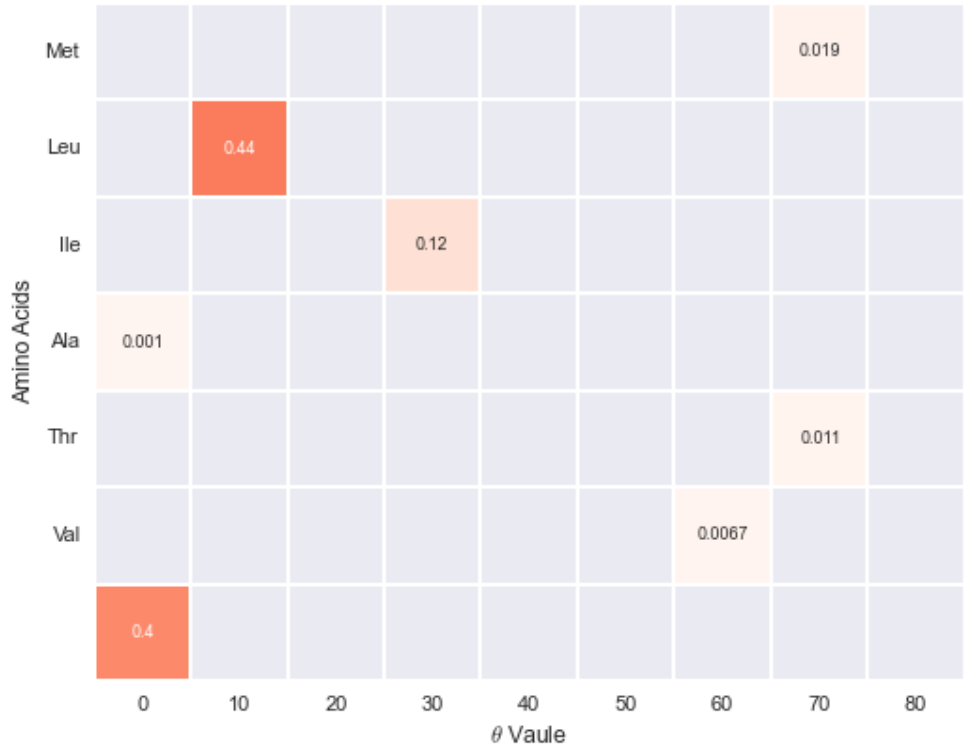

Figure 6.2: Return composition of Case 2 for one random run of the test case set with scaling foctor for mixed amino acids, with θ expanded from 0° to 80°. More detailed data of this target composition can be found in Appendix A.5.

scaling factors of these two spectroscopy techniques.

6.2.2 Test Cases with Scaling Factor Considering Each Amino Acid Candidates from 0° to 180° on θ

When each amino acid's candidates are expanded from 0° to 180° on θ, the same test case set is applied 100 times with randomly generated scaling factors in each run. The test case result from the 100 run illustrates that all test cases in the set meets the above observation with zero frequency.

However, when further analyze the return compositions of Case 2 and 6, there are few other observations to be noted. To facilitate the explanation, one random run is picked as an explicit example. Figure 6.4 is the target composition. Figure 6.5 and Figure 6.6 are the return compositions of Case 2 and Case 6. The generated scaling

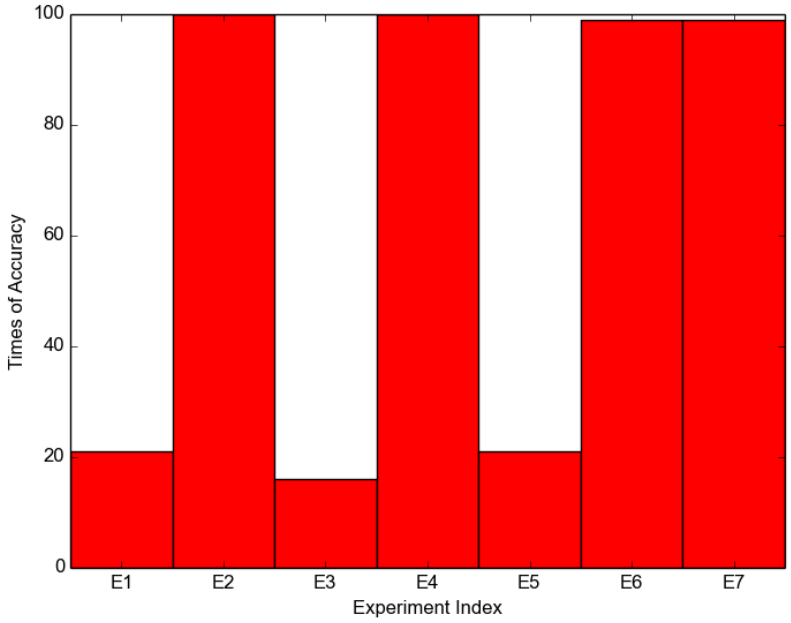

Figure 6.3: Test case accuracy analysis for test cases using experimental spectra data that contains scaling factor that is smaller than 1 and candidates with θ from 0° to 80°

factor for IR, Raman and SFG are 0.863411, 0.770505 and 0.239947.

In Figure 6.5, in the return composition of Case 2, the slack variable equals $1 - SF = 1 - 0.77 = 0.23$. For each amino acid, the selected candidate in the return composition may not be the exact one as shown in the target composition. However, this selected candidate is always either the correct one, or the correct one's θ complimentary. Moreover, the ratios between the percentage of each selected candidate in Figure 6.5 and Figure 6.4 are the same as shown in Equation 6.2 (more precise calculated can be found in Appendix A.10). These ratios all equal to the scaling factor of Raman.

In Figure 6.5, for each amino acid, there are two selected candidates in the return composition. These two selected candidates are the correct one and its θ complimentary. When the percentages of these two selected candidates are added, it equals to the percentage returned for the amino acid in Figure 6.4. $0.27 + 0.14 = 0.41$. Between these two selected candidates, the correct one's percentage is always bigger than its

θ complement. $0.27 > 0.14$. In conclusion, Case 2 achieves in telling the slack variable, the scaling factor, and the ratio between the returned candidates and the target ones. However, in order to distinguish the exact candidate of each amino acid, the extra information from Case 6 is required. Case 6 tells the correct candidate from its complement on θ. Together with the return information from Case 2 and 6, the target composition can be obtained. These observations can be applied to every run of the test case set.

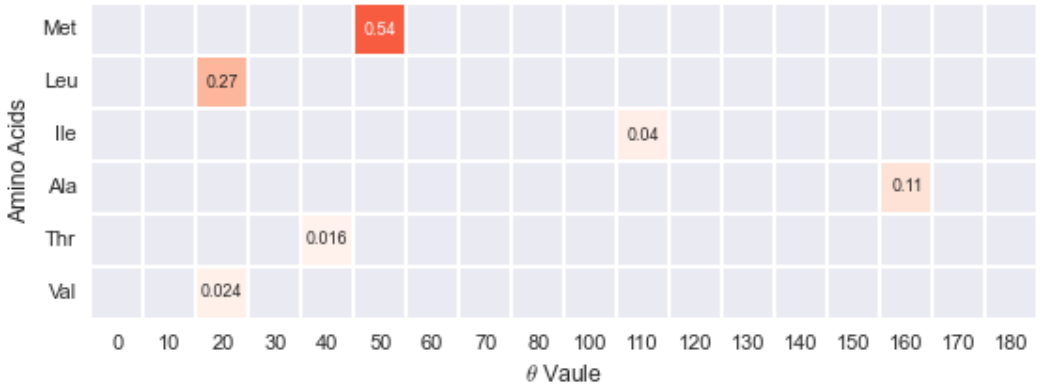

Figure 6.4: Target composition of one random run of test cases containing scaling factor and the mixed amino acids' candidates with θ expended from 0° to 180°. More detailed data of this target composition can be found in Appendix A.6.

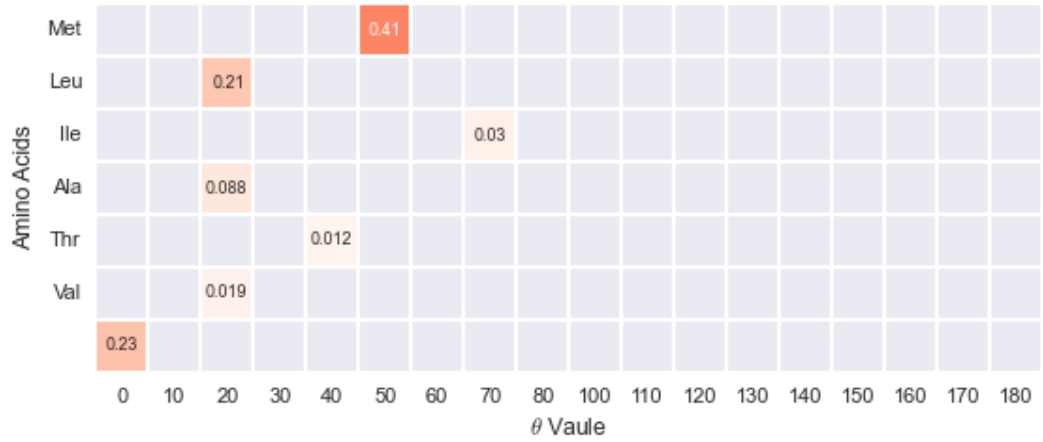

Figure 6.5: Return composition of Case 2 for one random run of test cases containing scaling factor and the mixed amino acids' candidates with θ expended from 0° to 180°. More detailed data of this target composition can be found in Appendix A.7.

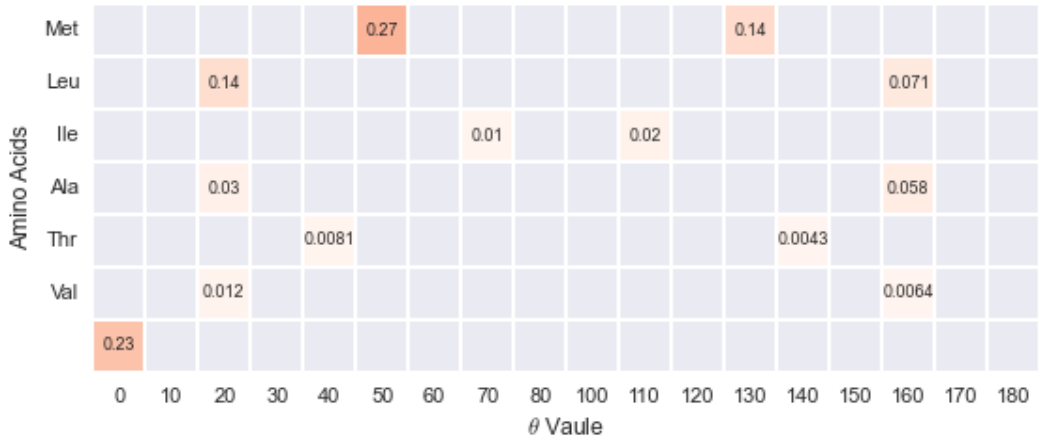

Figure 6.6: Return composition of Case 6 for one random run of test cases containing scaling factor and the mixed amino acids' candidates with θ expended from 0° to 180°. More detailed data of this target composition can be found in Appendix A.8.

$$\frac{0.41}{0.54} = \frac{0.21}{0.27} = \frac{0.03}{0.04} = \frac{0.088}{0.11} = \frac{0.012}{0.016} = \frac{0.019}{0.024} = 0.77 \tag{6.2}$$

6.3 Conclusion

With Scaling factor introduced to different spectroscopy techniques, Raman spectral information alone is sufficient to obtain the target composition, when considering a mixture of amino acids with candidates expanded from 0° to 80° on θ. The target composition can be re-constructed from the return SV and composition. The SF equals 1 minus SV.

When each amino acid's candidates are expanded from 0° to 180°, both return compositions from Case 2 and 6 are needed to obtain the target composition.

Chapter 7

Conclusion and Future Work

7.1 Conclusion

In addition to existing two common approaches in studying the possible composition of candidates of model spectra, the use of LP has been explored by Hung [4]. It has been approved that LP can solve this problem in pseudo polynomial time $O(n)$, which is much better than the two existing approaches in computational gain. However, the reason why the LP model does not always return the target composition of mock spectra was unknown. The first goal of this study is to figure out this reason.

The achieve the first goal, a simplified molecular model is designed to analyze the nature of the LP model. It has shown that as long as there is the right data set, the target composition is obtained. If the target composition is not returned correctly, then there is not sufficient spectral information to describe the test cases to the LP model

Furthermore, I apply all the spectral information of a realistic molecule (Met) to the LP model, it is not guaranteed to return the target composition all the time. The spectral information we collect is not sufficient in describing the test cases to the LP model most of the time.

Following the scenario of having one type of realistic molecule at surfaces, the test cases of having multiple types of realistic molecules at surface are also explored. When each molecule's candidates expanded from 0° to 80° on θ, Raman or SFG spectral

information alone is sufficient to obtain the target composition. When the candidates are expanded from 0° to 180° on θ, SFG spectral information needs to combine with IR or Raman in order to obtain the target composition.

At last, instead of generating the target spectra by combining different candidates directly, they are obtained from real experimental data. Therefore, for each spectroscopy technique, there is a scaling factor between the candidate spectra generated theoretically and the real experimental target spectra. When consider a mixture of realistic molecules with candidates expanded from 0° to 80° on θ, Raman spectral information alone is sufficient to obtain the target composition. Because the target composition can be re-constructed from the return SV and composition. The SF equals 1 minus SV. When each realistic molecule's candidates are expanded from 0° to 180°, both return compositions of using only Raman spectral information and using Raman and SFG spectral information are needed to obtain the target composition.

7.2 Future Work

Our LP model has proven its efficiency in studying molecular orientation distribution at surfaces when different molecules are considered. However, when considering one type of molecule at the surface, there is not enough spectral information for the LP model to obtain the target composition. One of the most important direction is to collect more spectral information to the LP model. Another direction is to combine LP technique with other computation model to further constraint the solution space of the target composition.

Appendix A

Additional Information

Detailed data value for Figure 5.4

$$\begin{bmatrix}
0 & 0 & 0 & 0 & 0 & 0 & 0 & 0 & 0 & 0 & 0 & 0.299586 & 0 & 0 & 0 & 0 & 0 & 0 \\
0 & 0 & 0 & 0.664053 & 0 & 0 & 0 & 0 & 0 & 0 & 0 & 0 & 0 & 0 & 0 & 0 & 0 & 0 \\
0 & 0 & 0 & 0 & 0 & 0 & 0 & 0 & 0 & 0 & 0 & 0 & 0 & 0 & 0 & 0 & 0.021196 & 0 \\
0 & 0 & 0 & 0 & 0 & 0 & 0 & 0 & 0.00662804 & 0 & 0 & 0 & 0 & 0 & 0 & 0 & 0 & 0 \\
0 & 0 & 0 & 0 & 0 & 0 & 0 & 0 & 0 & 0 & 0 & 0 & 0.000642609 & 0 & 0 & 0 & 0 & 0 \\
0 & 0 & 0 & 0 & 0 & 0 & 0 & 0 & 0 & 0 & 0 & 0 & 0.00789 & 0 & 0 & 0 & 0 & 0
\end{bmatrix} \tag{A.1}$$

Detailed data value for Figure 5.5

$$\begin{bmatrix}
0 & 0 & 0 & 0 & 0 & 0 & 0.299586 & 0 & 0 & 0 & 0 & 0 & 0 & 0 & 0 & 0 & 0 \\
0 & 0 & 0 & 0.664053 & 0 & 0 & 0 & 0 & 0 & 0 & 0 & 0 & 0 & 0 & 0 & 0 & 0 \\
0 & 0.021196 & 0 & 0 & 0 & 0 & 0 & 0 & 0 & 0 & 0 & 0 & 0 & 0 & 0 & 0 & 0 \\
0 & 0 & 0 & 0 & 0 & 0 & 0 & 0 & 0.00662804 & 0 & 0 & 0 & 0 & 0 & 0 & 0 & 0 \\
0 & 0 & 0 & 0 & 0 & 0.000642609 & 0 & 0 & 0 & 0 & 0 & 0 & 0 & 0 & 0 & 0 & 0 \\
0 & 0 & 0 & 0 & 0 & 0.00789 & 0 & 0 & 0 & 0 & 0 & 0 & 0 & 0 & 0 & 0 & 0
\end{bmatrix} \tag{A.2}$$

Detailed data value for Figure 5.6

$$\begin{bmatrix}
0 & 0 & 0 & 0 & 0 & 0 & 0 & 0 & 0 & 0 & 0 & 0.299586 & 0 & 0 & 0 & 0 & 0 & 0 \\
0 & 0 & 0 & 0.664053 & 0 & 0 & 0 & 0 & 0 & 0 & 0 & 0 & 0 & 0 & 0 & 0 & 0 & 0 \\
0 & 0 & 0 & 0 & 0 & 0 & 0 & 0 & 0 & 0 & 0 & 0 & 0 & 0 & 0 & 0 & 0.021196 & 0 \\
0 & 0 & 0 & 0 & 0 & 0 & 0 & 0 & 0.00662804 & 0 & 0 & 0 & 0 & 0 & 0 & 0 & 0 & 0 \\
0 & 0 & 0 & 0 & 0 & 0 & 0 & 0 & 0 & 0 & 0 & 0 & 0.000642609 & 0 & 0 & 0 & 0 & 0 \\
0 & 0 & 0 & 0 & 0 & 0 & 0 & 0 & 0 & 0 & 0 & 0 & 0.00789 & 0 & 0 & 0 & 0 & 0
\end{bmatrix} \tag{A.3}$$

Detailed data value for Figure 6.1

$$\begin{bmatrix} 0 & 0 & 0 & 0 & 0 & 0 & 0 & 0.03218 & 0 \\ 0 & 0.73929 & 0 & 0 & 0 & 0 & 0 & 0 & 0 \\ 0 & 0 & 0 & 0.19745 & 0 & 0 & 0 & 0 & 0 \\ 0.00173 & 0 & 0 & 0 & 0 & 0 & 0 & 0 & 0 \\ 0 & 0 & 0 & 0 & 0 & 0 & 0 & 0.01819 & 0 \\ 0 & 0 & 0 & 0 & 0 & 0 & 0.01116 & 0 & 0 \end{bmatrix} \tag{A.4}$$

Detailed data value for Figure 6.2

$$\begin{bmatrix} 0 & 0 & 0 & 0 & 0 & 0 & 0 & 0.019308 & 0 \\ 0 & 0.443574 & 0 & 0 & 0 & 0 & 0 & 0 & 0 \\ 0 & 0 & 0 & 0.11847 & 0 & 0 & 0 & 0 & 0 \\ 0.001038 & 0 & 0 & 0 & 0 & 0 & 0 & 0 & 0 \\ 0 & 0 & 0 & 0 & 0 & 0 & 0 & 0.010914 & 0 \\ 0 & 0 & 0 & 0 & 0 & 0 & 0.006696 & 0 & 0 \\ 0.4 & & & & & & & & \end{bmatrix} \tag{A.5}$$

Detailed data value for Figure 6.4. Target composition

$$\begin{bmatrix} 0 & 0 & 0 & 0 & 0.53762 & 0 & 0 & 0 & 0 & 0 & 0 & 0 & 0 & 0 & 0 & 0 \\ 0 & 0 & 0.26894 & 0 & 0 & 0 & 0 & 0 & 0 & 0 & 0 & 0 & 0 & 0 & 0 & 0 \\ 0 & 0 & 0 & 0 & 0 & 0 & 0 & 0 & 0 & 0.03951 & 0 & 0 & 0 & 0 & 0 & 0 \\ 0 & 0 & 0 & 0 & 0 & 0 & 0 & 0 & 0 & 0 & 0 & 0 & 0 & 0.11382 & 0 & 0 \\ 0 & 0 & 0 & 0 & 0.01604 & 0 & 0 & 0 & 0 & 0 & 0 & 0 & 0 & 0 & 0 & 0 \\ 0 & 0 & 0.02407 & 0 & 0 & 0 & 0 & 0 & 0 & 0 & 0 & 0 & 0 & 0 & 0 & 0 \end{bmatrix} \tag{A.6}$$

Detailed data value for Figure 6.5. Return composition of Result 2

$$\begin{bmatrix} 0 & 0 & 0 & 0 & 0 & 0.414239 & 0 & 0 & 0 & 0 & 0 & 0 & 0 & 0 & 0 & 0 & 0 \\ 0 & 0 & 0.20722 & 0 & 0 & 0 & 0 & 0 & 0 & 0 & 0 & 0 & 0 & 0 & 0 & 0 & 0 \\ 0 & 0 & 0 & 0 & 0 & 0 & 0 & 0.0304427 & 0 & 0 & 0 & 0 & 0 & 0 & 0 & 0 & 0 \\ 0 & 0 & 0.0876989 & 0 & 0 & 0 & 0 & 0 & 0 & 0 & 0 & 0 & 0 & 0 & 0 & 0 & 0 \\ 0 & 0 & 0 & 0 & 0.0123589 & 0 & 0 & 0 & 0 & 0 & 0 & 0 & 0 & 0 & 0 & 0 & 0 \\ 0 & 0 & 0.0185461 & 0 & 0 & 0 & 0 & 0 & 0 & 0 & 0 & 0 & 0 & 0 & 0 & 0 & 0 \\ 0.229495 & 0 & 0 & 0 & 0 & 0 & 0 & 0 & 0 & 0 & 0 & 0 & 0 & 0 & 0 & 0 & 0 \end{bmatrix} \tag{A.7}$$

Detailed data value for Figure 6.6. Return composition of Result 6

$$\begin{bmatrix} 0 & 0 & 0 & 0 & 0 & 0.27162 & 0 & 0 & 0 & 0 & 0 & 0 & 0.142619 & 0 & 0 & 0 & 0 & 0 \\ 0 & 0 & 0.135875 & 0 & 0 & 0 & 0 & 0 & 0 & 0 & 0 & 0 & 0 & 0 & 0 & 0.0713442 & 0 & 0 \\ 0 & 0 & 0 & 0 & 0 & 0 & 0 & 0.0104812 & 0 & 0 & 0.0199615 & 0 & 0 & 0 & 0 & 0 & 0 & 0 \\ 0 & 0 & 0.0301941 & 0 & 0 & 0 & 0 & 0 & 0 & 0 & 0 & 0 & 0 & 0 & 0 & 0.0575048 & 0 & 0 \\ 0 & 0 & 0 & 0 & 0.00810383 & 0 & 0 & 0 & 0 & 0 & 0 & 0 & 0 & 0.00425508 & 0 & 0 & 0 & 0 \\ 0 & 0 & 0.0121608 & 0 & 0 & 0 & 0 & 0 & 0 & 0 & 0 & 0 & 0 & 0 & 0 & 0.00638527 & 0 & 0 \\ 0.229495 & 0 & 0 & 0 & 0 & 0 & 0 & 0 & 0 & 0 & 0 & 0 & 0 & 0 & 0 & 0 & 0 & 0 \end{bmatrix} \tag{A.8}$$

$$\frac{0.019308}{0.03218} = \frac{0.443574}{0.73929} = \frac{0.11847}{0.19745} = \frac{0.001038}{0.00173} = \frac{0.010914}{0.01819} = \frac{0.006696}{0.01116} = 0.6 \quad \text{(A.9)}$$

$$\frac{0.414239}{0.53762} = \frac{0.20722}{0.26894} = \frac{0.0304427}{0.03951} = \frac{0.0876989}{0.11382} = \frac{0.0123589}{0.01604} = \frac{0.0185461}{0.02407} = 0.770505 \quad \text{(A.10)}$$

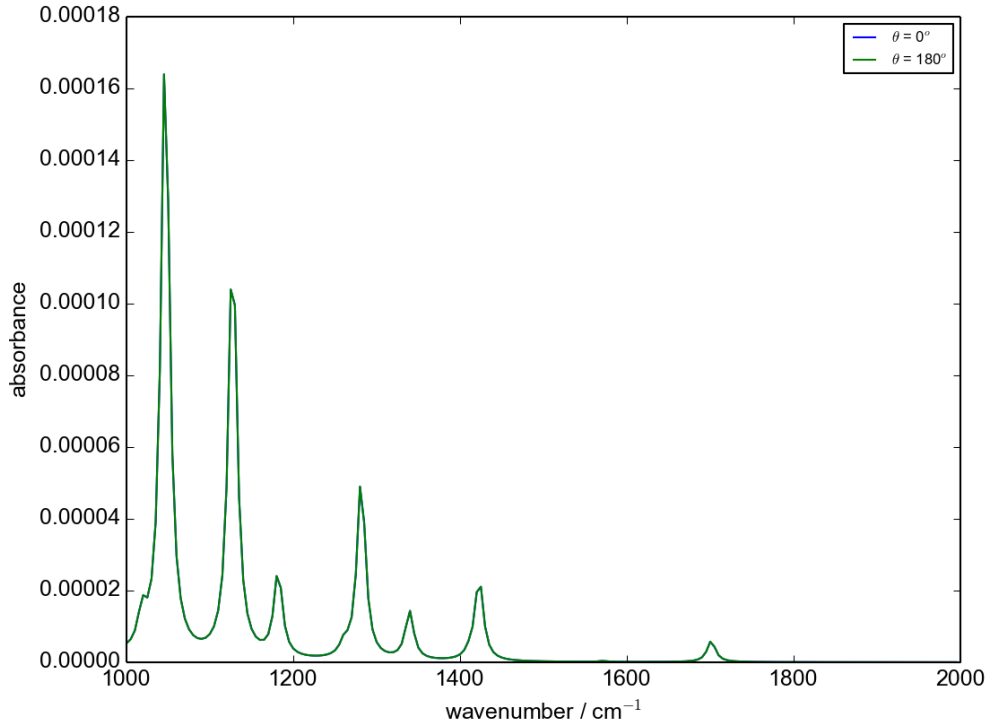

Figure A.1: IR z projection spectrum for alanine candidate with θ of 0° is identical to alanine candidate with θ of 180°

Number of Candidates	5	
Candidates	[0, 10, 20, 30, 40]	
Target Composition	[0.2, 0.2, 0.2, 0.2, 0.2]	
Test case index	Constraints	Result
10	200 x 200 z	[0.607766, 0, 0, 0, 0.392234]
11	200 xx 200 xy 200 xz 200 zz	[0.247792, 0, 0.502139, 0, 0.250069]
12	200 xxz 200 xzx 200 zzz	[0.321014, 0, 0.31018, 0.163041, 0.205764]
13	200 x 200 z 200 xx 200 xy 200 xz 200 zz	[0.247792, 0, 0.502139, 0, 0.250069]
14	200 xx 200 xy 200 xz 200 zz 200 xxz 200 xzx 200 zzz	[0.321014, 0, 0.31018, 0.163041, 0.205764]
15	200 x 200 z 200 xxz 200 xzx 200 zzz	[0.321014, 0, 0.31018, 0.163041, 0.205764]
16	200 x 200 z 200 xx 200 xy 200 xz 200 zz 200 xxz 200 xzx 200 zzz	[0.321014, 0, 0.31018, 0.163041, 0.205764]

Table A.1: More precise result data of Test Case 10 to 16 setting for methionine candidates

# Candidates	9	
Candidates	[0, 10, 20, 30, 40, 50, 60, 70, 80]	
Target Composition	[0.2201, 0.28905, 0.05201, 0.08251, 0.35633, 0, 0, 0, 0]	
Test Case #	# of Data Points	Result Composition
17	each 5 wavenumber of IR, Raman and SFG spectra	[0.158921, 0.388434, 0.0, 0.0985466, 0.354099, 0.0, 0.0, 0.0, 0.0]
18	each 500 wavenumber of IR, Raman and SFG spectra	[0.397991, 0.0, 0.203394, 0.0357663, 0.362848, 0.0, 0.0, 0.0, 0.0]

Table A.2: More precise result data of Test case 17 and 18 to explain the limitation of our LP model for methionine molecule

Test Case #	# Data Points	Points Selection	Return Composition
6	10	[2800, 3300, 50], z	[0, 0.796962, 0.103038, 0.1]
7	20	[2800, 3300, 25], z	[0, 0.796962, 0.103038, 0.1]
8	25	[2800, 3300, 20], z	[0, 0.796962, 0.103038, 0.1]
9	32	[2800, 3300, 15], z	[0, 0.796962, 0.103038, 0.1]
10	50	[2800, 3300, 10], z	[0, 0.796962, 0.103038, 0.1]
11	100	[2800, 3300, 5], z	[0, 0.796962, 0.103038, 0.1]
12	$100 + 1$	[2800, 3300, 5], z [2800, 3300, 500], x	[0, 0.796962, 0.103038, 0.1]
13	$100 + 5$	[2800, 3300, 20], z [2800, 3300, 100], x	[0, 0.796962, 0.103038, 0.1]
14	$100 + 10$	[2800, 3300, 20], z [2800, 3300, 50], x	[0, 0.796962, 0.103038, 0.1]
15	$100 + 50$	[2800, 3300, 20], z [2800, 3300, 10], x	[0.1, 0.5, 0.4, 0]
16	$100 + 100$	[2800, 3300, 20], z [2800, 3300, 5], x	[0.1, 0.5, 0.4, 0]

Table A.3: Constraint study based on Case 4 of simplified molecule.

Test Case #	# of Data Points	Point Selection	Return Composition
17	10	[2800, 3300, 50], z	[0.156758, 0, 0, 0.825977, 0, 0, 0, 0, 0, 0.017265]
18	25	[2800, 3300, 20], z	[0, 0, 0.730541, 0, 0.212061, 0, 0, 0.0573978, 0, 0, 0]
19	50	[2800, 3300, 10], z	[0, 0, 0.730541, 0, 0.212061, 0, 0, 0.0573978, 0, 0, 0]
20	100	[2800, 3300, 5], z	[0, 0, 0.730541, 0, 0.212061, 0, 0, 0.0573978, 0, 0, 0]
21	500	[2800, 3300, 1], z	[0, 0, 0.730541, 0, 0.212061, 0, 0, 0.0573978, 0, 0, 0]
22	100 + 1	[2800, 3300, 5], z [2800, 3300, 500], x	[0, 0, 0.730541, 0, 0.212061, 0, 0, 0.0573978, 0, 0, 0]
23	100 + 10	[2800, 3300, 5], z [2800, 3300, 50], x	[0.361587, 0, 0.312061, 0.326352, 0, 0, 0, 0, 0]
24	100 + 20	[2800, 3300, 5], z [2800, 3300, 25], x	[0.174023, 0, 0, 0.791447, 0, 0, 0.0345301, 0, 0, 0]
25	100 + 25	[2800, 3300, 20], z [2800, 3300, 20], x	[0.174023, 0, 0, 0.791447, 0, 0, 0.0345301, 0, 0, 0]
26	100 + 50	[2800, 3300, 5], z [2800, 3300, 10], x	[0, 0, 0.753209, 0, 0.146791, 0, 0.1, 0, 0, 0]
27	100 + 84	[2800, 3300, 5], z [2800, 3300, 6], x	[0.174023, 0, 0, 0.791447, 0, 0, 0.0345301, 0, 0, 0]
28	100 + 100	[2800, 3300, 5], z [2800, 3300, 5], x	[0.1, 0, 0.5, 0, 0.4, 0, 0, 0, 0, 0]

Table A.4: Constraint study based on Case 5 of simplified molecule.

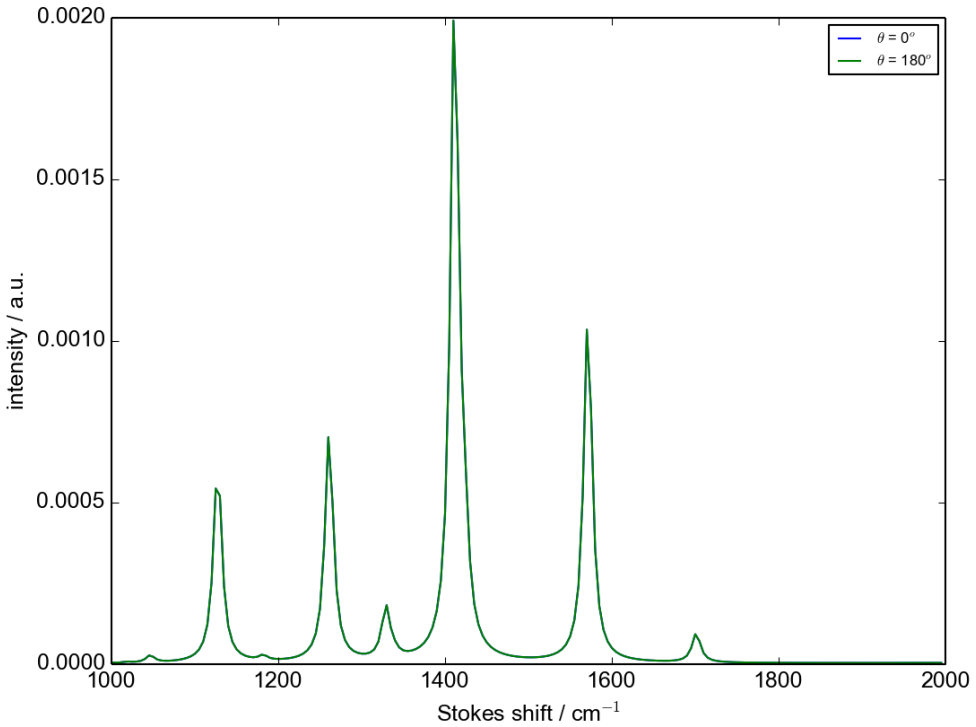

Figure A.2: Raman zz projection spectrum for alanine candidate with θ of 0° is identical to alanine candidate with θ of 180°

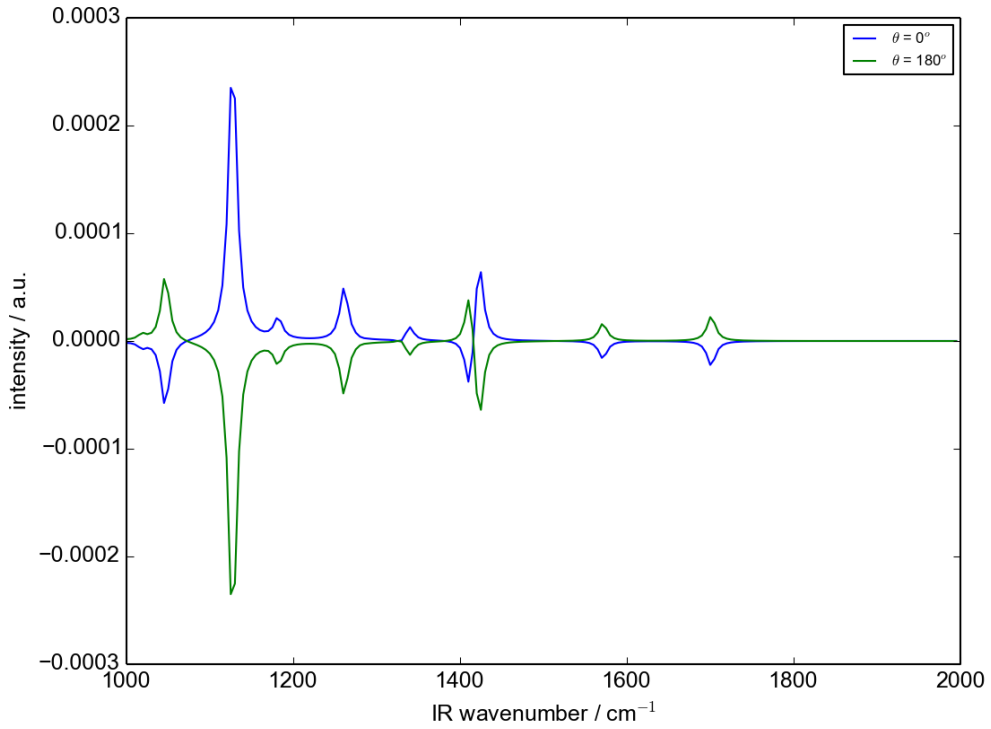

Figure A.3: SFG zzz projection spectrum for alanine candidate with θ of 0° is not identical to alanine candidate with θ of 180°, but symmetric along wavelength

Bibliography

[1] Stephen Boyd and Lieven Vandenberghe. *Convex Optimization*. Cambridge University Press New York, NY, USA, 2004.

[2] Sophie Brasselet. Polarization-resolved nonlinear microscopy: application to structural molecular and biological imaging. *Adv. Opt. Photon.*, 3(3):205, Sep 2011.

[3] Vasek Chvatal. *Linear Programming*. W. H. Freeman and Company, 1983.

[4] Kuo Kai Hung. Extracting surface structural information from vibrational spectra with linear programming. Master's thesis, University of Victoria, 2015.

[5] Jiri Maousek and Bernd Cartner. *Understanding and Using Linear Programming*. Springer, 2007.

[6] M.W.Schmidt, K.K.Baldridge, J.A.Boatz, S.T.Elbert, M.S.Gordon, J.H.Jensen, S.Koseki, N.Matsunaga, K.A.Nguyen, S.J.Su, T.L.Windus, M.Dupuis, and J.A.Montgomery. *General Atomic and Molecular Electronic Structure System*. Department of Chemistry Iowa State University, July 2016.

[7] Roy Sandra, Hung Kuo-Kai, Stege Ulrike, and K.Hore Dennis. Rotations, projections, direction cosines, and vibrational spectra. *Applied Spectroscopy Reviews*, 49:233–248, May 1999.

[8] Pratt Arnold W, Toal J. Nicolet, and Rushizky George W. Computer assisted analysis of oligonucleotides. *Annals of the New York Academy of Sciences*, 128(3):900–913, 1966.

[9] William C. Whiten, Marvin B. Shapiro, and Arnold W. Pratt. Linear programming applied to ultraviolet absorption spectroscopy. *Communications of the ACM*, 6:66–67, 1963.

[10] Zhuang X., Miranda P. B., Kim D., and Shen Y. R. Mapping molecular orientation and conformation at interfaces by surface nonlinear optics. *Phys. Rev. B*, 59:12632–12640, May 1999.